U.PORTO
FMUP FACULDADE DE MEDICINA UNIVERSIDADE DO PORTO

Is TRPV1 involved in pain and bladder dysfunction associated with multiple sclerosis?

An experimental study in the rat.

HELENA ISABEL ALVITES CAVALEIRO

DISSERTAÇÃO DE CANDIDATURA AO GRAU DE MESTRE APRESENTADA À FACULDADE DE MEDICINA DA UNIVERSIDADE DO PORTO

Mestrado em Neurobiologia

Orientador: Professora Doutora. Célia Duarte Cruz

Co-Orientador: Professor Doutor. Francisco Cruz

M
2017

FMUP – Departamento de Biomedicina

Dissertação apresentada à Universidade do Porto para cumprimento dos requisitos necessários à obtenção do grau de Mestre em Neurobiologia realizada sob a orientação científica da Doutora Célia Duarte Cruz, professora associada com agregação do Departamento de Biomedicina da Faculdade de Medicina da Universidade do Porto, onde esta tese foi realizada.

Dissertation submitted to the University of Porto to fulfill the requirements for obtaining the degree of Master in Neurobiology carried out under the scientific supervision of Célia Duarte Cruz PhD, associated professor at the Department of Biomedicine of the Faculty of Medicine of the University of Porto, where this thesis was developed.

Agradecimentos

Quando se diz “lá na terrinha”, que se estuda ou trabalha na faculdade de Medicina da Universidade do Porto, isso tem o seu impacto entre os demais. Aqui, apercebi-me que o sucesso que se vê de fora é o culminar de muito e que, por trás de “Um senhor professor Doutor” há muita coisa escondida. Aqui, apercebi-me que, deste lado, as pessoas são feitas de uma fibra diferente e ter-vos conhecido foi uma golfada de ar fresco. Para além da sua índole académica, este ano foi uma lição de vida e um abre olhos, para o que ainda aí vem. Foi ainda a certeza, de que, venha o que vier, não vou estar sozinha.

Obrigada professora Célia, pelo carinho, ensino e profissionalismo. Por não desistir de mim. Por me mostrar que na vida, tudo se consegue. Que, mesmo que a nossa vida pessoal esteja um caus, há coisas e pessoas com as quais nos comprometemos e que temos de cumprir dê por onde der, ainda que isso implique um pouco de mau humor pelo meio. É um exemplo a seguir.

Obrigada, aos outros elementos do grupo, Ana Coelho, Raquel Oliveira, Ana Charrua, Marília Torrado, pelos ensinamentos no laboratório. Pela paciência, pelas conversas, pelas risadas ou pela simples companhia. Foi um prazer. Obrigada, professor António Avelino, pelas dicas científicas nos nossos ‘Lab mettings´. Obrigada Elisa e Sr.Fernando.

Agradeço à professora Deolinda Lima, coordenadora deste Mestrado, a oportunidade e o facto, de sempre, lutar pelos direitos dos seus alunos.

Não posso esquecer todos os professores do Mestrado. Obrigada pelos ensinamentos. Destaco o professor Carlos Reguenga, que no início deste percurso de tudo fez para que nos integrássemos no Mestrado e nos orientou na tomada das melhores escolhas.

Um grande obrigada a todos os colegas de Mestrado e Doutoramento. Obrigada Zé e Rita, pela ajuda no micrótomo e testes de comportamento. Por serem sempre tão prestáveis. Obrigada ao teu bom humor Zé, e à tua ternura Rita. Obrigada Raquel Silva, por seres a trintona mais fofa de sempre. Vais estar sempre no meu coração.

Obrigada Inês, Rita, Liliana, Zé Carlos e Sílvia. Um obrigada enorme para vocês. Foram o meu pilar a todos os níveis neste mestrado. Obrigada pelo companheirismo, compreensão e ajuda. Obrigada, meu menino Zé, por afinal seres um grande Homem. Obrigada Sílvia por seres a pessoa mais bonita que conheço. Nada seria igual se não tivesses aparecido. Obrigada. Um dia quero ser como tu.

Obrigada José, por me mostrares, nos momentos de desespero, que a minha vida não é assim tão má. Obrigada pela paciência e amor.

Obrigada aos meus pais, por me permitirem estar aqui. Espero um dia retribuir tudo o que têm feito por mim. Obrigada Tina e Zé por aturarem as minhas neuras de irmã mais velha.

Por fim, não menos importante, mas porque és parte de mim, muito obrigada Raquel Alonso. Obrigada por estes anos, pelas conversas, pelas risadas. Por me conheceres melhor que ninguém. Por tudo e por nada. Obrigada por estares comigo.

Tabble of contents

Listo of figures

Introduction

Results

EAE model induction, validation and characterization

Resiniferatoxin intrathecal injection

Abbreviations

BBB – Brain Blood Barrier

BoNT/A - Botulinum Neurotoxin Type A

CNS – Central Nervous System

DCM - Dorsal Commissure

DRG – Dorsal Root Ganglia

IC - Intermittent Catheterization

ILGs – Intermedio Lateral Grey matter Areas of the cord

IR – immunoreactive

LUT – Lower Urinary Tract

LUTD – Lower Urinary Tract Dysfunction

MOG - Myelin Oligodendrocyte Glycoprotein

MS – Multiple Sclerosis

MT – Mechanical threshold

Mts – Mechanical thresholds

Myelin Basic Protein – MBP

PWL – Paw whithrawal latency

PAG – Periaqueductal grey

PBS - phosphate buffer saline

PBST – phosphate buffer saline with 0.3% Triton X-100

PFA - paraformaldehyde

PLP - Proteolipid Proteins

PMC – Pontine Micturition Center

PRMS - Primary-Relapsing Multiple Sclerosis

RTX – Resineferatoxin toxinvanilloid 1

SPMS - secondary progressive Multiple Sclerosis

TRPV1 – Transient receptor potential

Sumário

Introdução: A Esclerose Múltipla é uma doença neurodegenerativa complexa e incapacitante (Lifson *et al.*), caraterizada por inflamação, desmielinização e gliose no sistema nervoso central. Os sintomas surgem aleatoriamente e são dependentes da área do sistema nervoso afetada. A dor crónica e a disfunção do trato urinário são dois dos severos sintomas que afetam a qualidade de vida dos pacientes. Relativamente ao último, podemos destacar a incontinência devida à hiperatividade neurogénica do músculo detrusor.

Objetivos e métodos: Estudos recentes sugerem o envolvimento do recetor de vanilóides, tipo 1 (TRPV1) na patofisiologia da esclerose múltipla (Paltser et al, 2013). O envolvimento do recetor nestes sintomas já se encontra descrito em modelos animais e na clínica (Szallasi *et al.*, 2006; Gunthorpe & Szallasi, 2008), no entanto, não é claro se o mesmo acontece quando estes sintomas estão associados à doença em estudo. Após indução do modelo animal de Encefalite Autoimune Experimental (EAE), os animais foram caraterizados em termos de desenvolvimento de dor e disfunção urinária durante o período de tempo experimental. A medula espinhal dos animais foi analisada por imunohistoquímica, com intuito de identificar sinais de desmielinização e de ativação de células gliais. O tecido foi, ainda, avaliado quanto à expressão de TRPV1, CGRP e IB4. Adicionalmente, um grupo de animais foi injetado com resinífera toxina (RTX) e outro com a solução veículo. O efeito das injeções intratecais foi avaliado a nível de sensibilidade cutânea e da função da bexiga.

Resultados: Os animais com indução da doença desenvolveram sensibilidade, mecânica e térmica, aumentadas, que oscilaram durante o período experimental. Também a função vesical se mostrou alterada nos animais EAE, tendo sido caracterizada por um aumento na frequência das contrações da bexiga e diminuição da amplitude. A análise do tecido mostrou perda de mielina no sistema nervoso central, sem que esta se tivesse verificado no Sistema Nervoso

Periférico. Células gliais da medula espinhal surgiram ativadas, enquanto a marcação de CGRP não mostrou alterações neste modelo animal. No que respeita à expressão de TRPV1, esta pareceu diminuída. A injeção intratecal de RTX aumentou a sensibilidade à estimulação mecânica, bem como trouxe melhorias na função da bexiga.

Conclusão: O presente estudo descreve alterações dinâmicas na sensibilidade cutânea num modelo animal de esclerose múltipla e de NDO. O TRPV1 surge como um possível participante na patofisiologia da esclerose múltipla e representa um alvo terapêutico para o alívio da sintomatologia.

Abstract

Background: Multiple sclerosis (Lifson et al.) is a complex and disabling neurodegenerative disease, characterized by inflammation, demyelination, axonal loss and gliosis at central nervous system. MS symptoms are random and disabling, depending on the affected area. Chronic pain and bladder dysfunction, particularly urinary incontinence to Neurogenic Detrusor Overactivity (NDO), two of the most bothersome MS symptoms reported by patients given their strong negative impact on daily tasks and quality of life.

Goals and methods: Recent studies have suggested the involvement of transient receptor potential vanilloid 1 (TRPV1) in MS pathophysiology (Paltser et al, 2013). While the contribution of this ion channel to chronic pain syndromes and bladder dysfunction has been established in various models of disease and in clinical context (Szallasi et al., 2006; Gunthorpe & Szallasi, 2008), it is not clear if the same happens in MS. Thus, the present study was designed to investigate if TRPV1 was implicated in pain and NDO during MS.

Here, we used an animal model of MS, the Experimental Autoimmune Encephalitis (EAE). Animals were characterized in terms of pain and bladder function during disease progression, followed by anaesthetized cystometry. Spinal cords were collected and analyzed by immunohistochemistry to identify signs of demyelination, glial activation, TRPV1 and CGRP expression and IB4 binding. Two other groups of EAE animals received intrathecal resiniferatoxin (RTX), a strong desensitizing TRPV1 agonist, or its vehicle and the effects on cutaneous sensitivity and bladder function assessed.

Results: EAE animals developed fluctuating heightened sensitivity to mechanical and hot stimulation during disease progression. Bladder function was also altered and EAE rats presented increased frequency of bladder reflex contractions, accompanied by a decrease in the amplitude of contractions. Tissue analysis showed signs of loss of myelin at the spinal cord but not in peripheral nerves. Spinal glia was also activated in sections from EAE rats. While spinal

CGRP was not altered by EAE, TRPV1 expression and IB4 binding were reduced. Intrathecal administration of RTX improved cutaneous sensitivity to mechanical stimulation and bladder function.

Conclusion: The present described the dynamic changes in cutaneous sensitivity in an animal model of MS and the emergence of NDO. As intrathecal RTX reduced both pain and bladder dysfunction, it is likely that TRPV1 is an important player in MS pathophysiology and may constitute an attractive therapeutic target to alleviate symptoms.

I. Introduction

I. Introduction

1. Multiple Sclerosis

Multiple sclerosis is one of the most common neurodegenerative diseases and affects millions of people worldwide (Trapp & Nave, 2008).This disorder is characterized by inflammation and fiber demyelination in the central nervous system (CNS) (Grigoriadis & van Pesch, 2015). With a strong economic and social impact MS has a higher prevalence in females and symptoms generally appear at an early age (20-40 years) (Bermel et al., 2010). While the exact etiology of MS is still not fully understood, it is believed that age, genetic and environmental factors may play a role in the induction of myelin degeneration on CNS (Franken et al., 2016).

Clinical manifestations of MS appear without warning and the clinical course is highly variable between affected individuals making treatment and prevention very difficult. Four different disorder subtypes have been recognized: relapsing-remitting MS (RRMS; with relapses of disease separated by periods without clinical progression or, in some cases, some recovery of function); primary-relapsing MS (PRMS); primary progressive MS (PPMS) and secondary progressive MS (SPMS). The most common MS subtype is RRMS, affecting 85-90% of patients, while PPMS is less frequent but presents the most severe neurological deterioration (Constantinescu et al., 2011).

Given the heterogeneity of symptoms (Figure 1) and variability of the time course of disease progression, a multidisciplinary approach is mandatory for the overall management of patients. Symptoms may occur as an outbreak when a lesion noticeably disrupts the nerve function, although the development of a lesion does not always lead to relapses (Giovannoni et al., 2016). Typically, the most common symptoms reported on the first visit to a clinician are abnormal cutaneous sensitivity to mechanical and thermal stimuli, fatigue, weakness and spasticity (Solaro & Uccelli, 2011). Other problems include vision problems such optic neuritis, diplopia and

nystagmus, dysphagia and breathing impairment related with loss of muscle strength and endurance. Importantly, the majority of patients present chronic pain (Seixas et al., 2014; Clemenzi et al., 2014) and detrusor overactivity that strongly affects their quality of life (Hennessey et al., 1999; Akkoc et al., 2016).

Most Common Symptoms	Less Common Symptoms
Fatigue	Speech disorders
Walking (gait), balance, and coordination problems	Swallowing problems
Bowel dysfunction	Headache
Dizziness and vertigo	Hearing loss
Pain	Seizures
Emotional changes	Tremor
Spasticity	Respiration/breathing problems
Numbness	Itching
Bladder dysfunction	
Vision problems	
Sexual dysfunction	
Cognitive dysfunction	
Depression	

***Figure 1**- Common symptoms for multiple sclerosis reported by patients (Based on information from National Multiple Sclerosis Society - http://www.nationalmssociety.org/about-multiple-sclerosis/what-we-know-about-ms/symptoms/indexaspx)*

1.1. Pathophysiological mechanisms of MS

While the precise etiology of MS is still to be fully understood, tissue damage is autoimmune in nature. There are four key pathological features of MS: inflammation, demyelination, axonal loss or damage and gliosis (Popescu et al., 2013). Impairment of the blood brain barrier (BBB), a neurovascular physical barrier composed by various cells that interact with each other and the neuronal parenchyma, is thought to be a key step (Neuwelt, 2004). Cells present in the BBB include pericytes, astrocytes, endothelial cells, and microglia. In normal conditions, tight junctions bind BBB cells and there is low vascular adhesiveness, which efficiently prevent extravasation of large and small solutes and prevents migration of any type of blood-borne cell. When the BBB is disrupted, a complex cascade of events is set in motion, during which BBB cells

become active and respond to mediators released either by neurons or by immune cells (Kebir et al., 2007). In MS, T-lymphocytes become activated in the periphery, cross the BBB membrane and attack CNS myelin sheaths. These T-cells are capable of producing inflammatory cytokines that further increase BBB permeability and attract other immune cells, such as B cells and monocytes/macrophages, to the CNS where they become active. These cells also release other inflammatory mediators, which contribute to an escalade and perpetuation of the inflammatory reaction (Figure 2). This exacerbated and localized inflammation at CNS leads to demyelination and gliosis (Constantinescu et al., 2011).

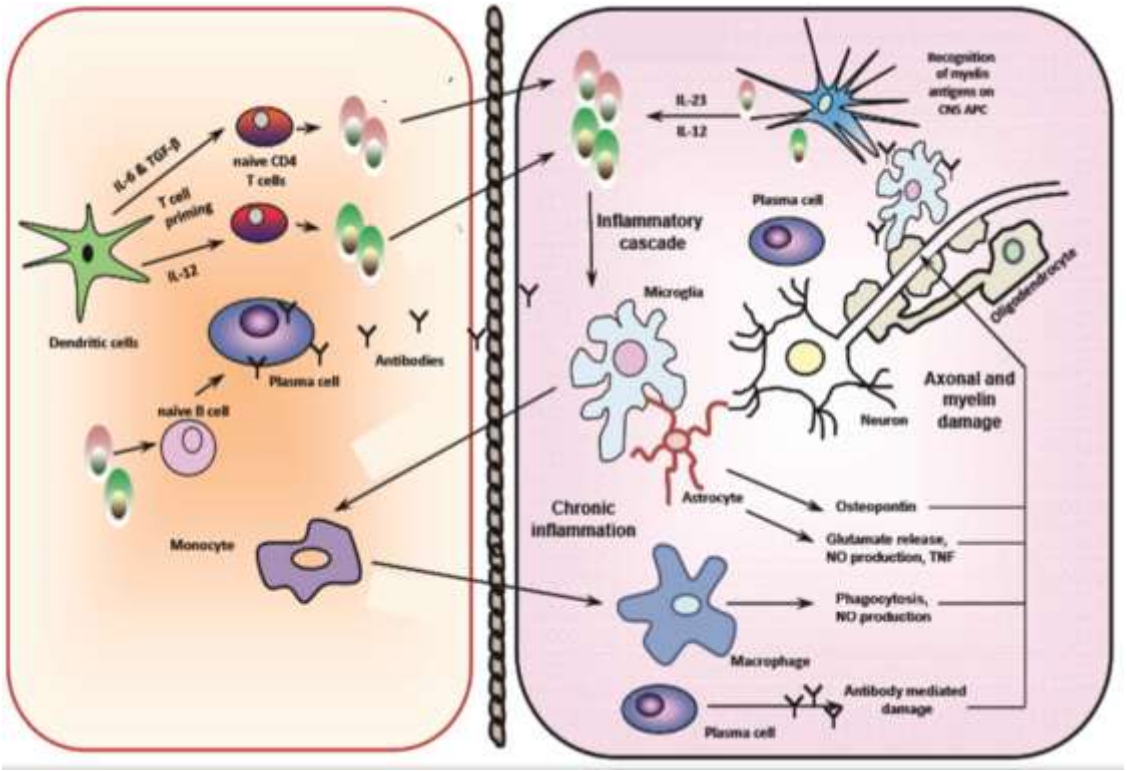

Figure 2 - Schematic diagram of some of the key pathological features of MS and EAE pathogenesis. *T lymphocytes are primed outside the CNS by dendritic cells. This T cells, then cross the blood–brain barrier and encounter CNS antigen-presenting cells. They produce inflammatory products and cytokines that damage the myelin and axons. They also activate the resident microglia and produce factors that attract further inflammatory cells to the CNS (Adapted from:Constantinescu et al., 2011).*

1.2. Experimental models of multiple sclerosis

Experimental autoimmune encephalomyelitis (EAE) is the most commonly used experimental animal model to study MS. Most EAE models present neuroinflammation, demyelination, and neuronal damage, which are key pathological characteristics of disease (Duffy et al., 2014). Importantly, EAE models are also able to mimic nociceptive behaviors, like thermal hyperalgesia and mechanical and cold allodynia (Aicher et al., 2004; Thibault et al., 2011), features that correlate with pain felt by MS patients. In rats and mice, EAE may be induced by immunizing the animals against myelin component such as myelin oligodendrocyte glycoprotein (MOG), myelin basic protein (MBP) and proteolipid proteins (PLP) (Constantinescu et al., 2011). Sensitization to myelin antigens in EAE typically occurs with the help of an adjuvant, usually containing bacterial components highly capable of activating the innate immune system via pattern recognition receptors (Libbey & Fujinami, 2011). The disease phenotype and histopathological features exhibited by each EAE-animal model symptoms depend upon the species, the specific myelin antigen, the immunization protocol utilized and the type of adjuvant used in the immunization protocol (Constantinescu et al., 2011).

2. Pain

2.1. Nociception

According to the International Association for the Study of Pain (IASP), pain is defined as an unpleasant sensory and emotional experience associated with actual or potential tissue damage, or described in terms of such damage. In most cases, pain arises after stimulation of nociceptors, which are peripheral sensory neurons that are sensitive to noxious stimuli (Snider & McMahon, 1998). Nociceptors have their cell bodies located in dorsal root ganglia (DRG) and extend peripheral branches to the skin, muscle, joints and visceral organ and central processes that terminate in the laminae I-II and deep dorsal horn of the spinal cord (Hunt & Mantyh, 2001;

Basbaum et al., 2009). These peripheral neurons are categorized into A-δ and C-fibres, according to their diameter and transmission velocity (Julius & Basbaum, 2001; Basbaum et al., 2009). Upon noxious stimulation, A-δ fibres are quickly activated and followed by C-fibres (Hunt & Mantyh, 2001), resulting in the release of neurotransmitters and neuropeptides in the spinal cord and activation of spinal neurons, located in the superficial laminae and lamina V. These neurons are responsible for conducting the information to the brain via spinothalamic and spinoreticulothalamic tracts, which carry pain messages to the thalamus and brainstem, respectively (Figure 3).

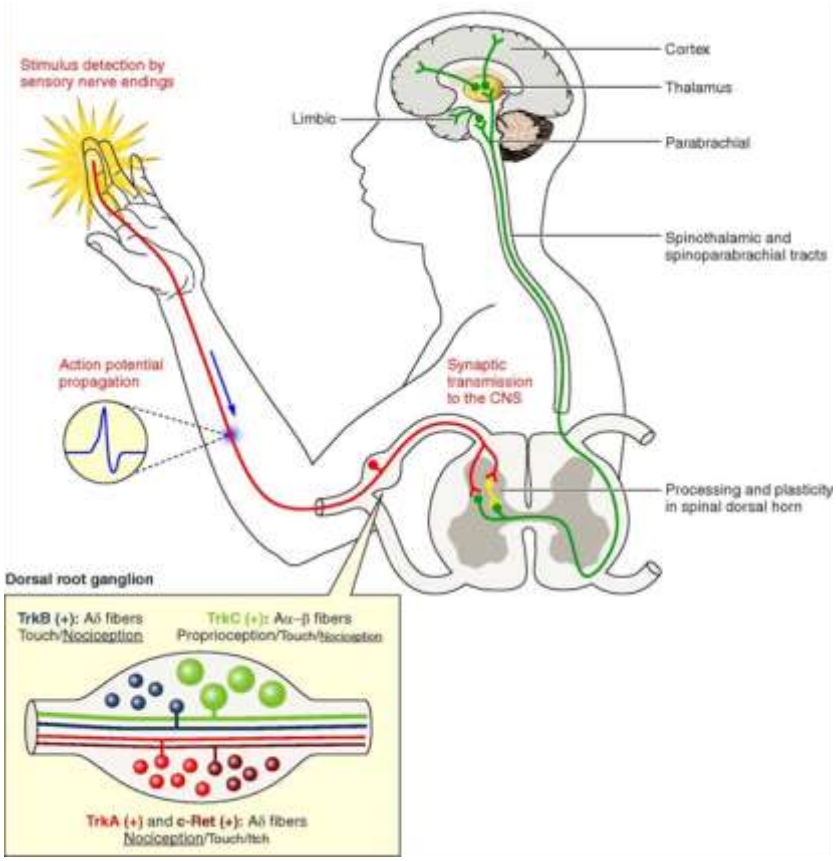

Figure 3-Brain Pain Networks. *Pain sensing neurons have a peripheral axon innervating the distal territories (skin, viscera, etc.) where they detect painful stimuli. Pain detection lead to an action potential that travels along the fibers up to the dorsal root ganglion (DRG) and then to the dorsal spinal cord. The sensory information is processed within the dorsal horn of the spinal cord before being sent to the thalamus to convey nociceptive information. Sensory neurons within the DRGs can be separated in positive small diameter sensory afferents (unmyelinated C-fibers) and larger diameter afferents (myelinated A-δ and A-α/β fibers) (Bourinet et al., 2014)*

More recently, attention has focused on spinal cord projections to the parabrachial region of the dorsolateral pons, connected with the amygdala, a region generally considered to process information relevant to the aversive properties of the pain experience (Julius & Basbaum, 2001; Basbaum et al., 2009). From these brainstem and thalamic loci, information reaches cortical groups of neurons located in the somatosensory cortex, the anterior cingulate gyrus, the insula and the pre-frontal cortex (Basbaum et al., 2009; Neugebauer et al., 2009). These cortical structures will then activate descending controls that regulate positively and negatively the transmission of pain messages at the level of the spinal cord (Heinricher et al., 2009).

2.2. Pain in Multiple sclerosis

It is widely accepted that pain is one of most unpleasant and disabling symptoms that interferes in MS patients' life, with a prevalence of 50-85% (Archibald et al., 1994; Svendsen et al., 2003). Pain reported by MS patients is typically characterized as neuropathic in nature, resulting from demyelination and inflammation within the CNS. Pain can also arise due to malposition-induced burden of joints and muscles and painful dysesthesias as well as visceral pain (Newland et al., 2009). Importantly, these painful complains often occur simultaneously.

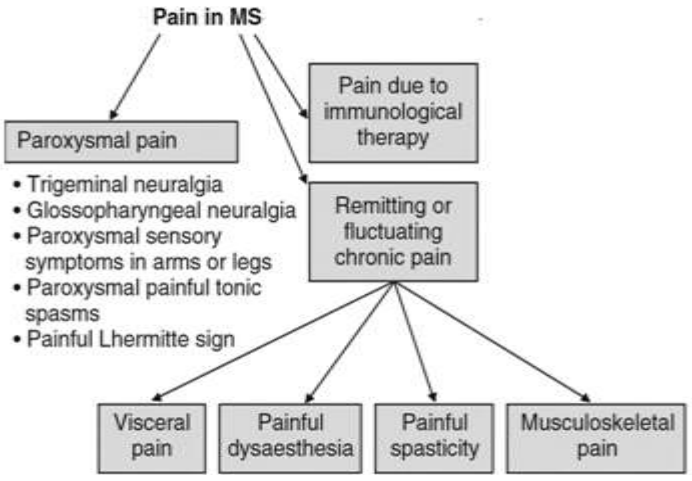

Figure 4 *- **Pain causes in multiple sclerosis.** Patients with MS may experience more than one pain syndrome alone or in combination, that could result from the disease or came as a secondary effect due to pain treatments applied. Adapted from (Pollmann & Feneberg, 2008).*

2.3. Astrocytes and microglia role in neuropathic pain

Neuropathic pain is characterized by pain in the absence of a stimulus or with normally innocuous stimuli, resulting from damage of the nervous system. (Edwards, 2005; Kaufmann et al., 2005). This type of pain results from a complex functional interaction between neurons, immune and glial cells in response to peripheral nerve injury (Scholz & Woolf, 2007). While mechanisms of central neuropathic are still not fully understood, peripheral neuropathic pain has been better studied. Following nerve injury, neuroinflammation is triggered at injury site. Immunoactive substances released at the site of injury initiate an immune response, by inducing the expression of surface antigens leading to the infiltration of immune cells to the site of injury (Jha et al., 2012; Chang et al., 2009; Kielian & Esen, 2004). Afterwards, perivascular microglia and astrocytes from spinal cord and brain are activated (Chang et al., 2013; Ellis & Bennett, 2013). Microglia are stimulated to proliferate and undergo profound morphological changes. These cells are responsible for the production of proinflammatory markers and cytokines, such as IL-1α and β, TNF-α, IL-6 and -12, fractalkine, and macrophage inflammatory protein 1α and β. Nitric oxide (NO), and reactive oxygen and nitrogen species are also released by activated microglia. Whereas microglia cells have a role in neuropathic pain at initial stages of pain progression, astrocytes are important to sustain pain sensation trough the time and its activity is closely associated with neurons and blood vessels (Watson & Frank, 2013). Like microglia, these glial cells undergo changes in gene expression upon inflammation, express higher levels of glial fibrillary acidic protein (GFAP) and increase the production of cytokines such as TNF-α and IL-1β (Didier et al., 1986). Activated astrocytes also secrete NO, excitatory amino acids, prostaglandins and ATP that mediate central sensitization, necessary for the development of chronic pain. Once astrocytes are activated, a phenomenon called calcium-wave, characterized by an increase in the cytosolic Ca^{2+} and its propagation among astrocytes, occurs. By propagated astrocytic calcium waves, the distant microglia become activated, leading to pain perception in regions distant from the original wound (Nedergaard & Dirnagl, 2005) (Figure. 5).

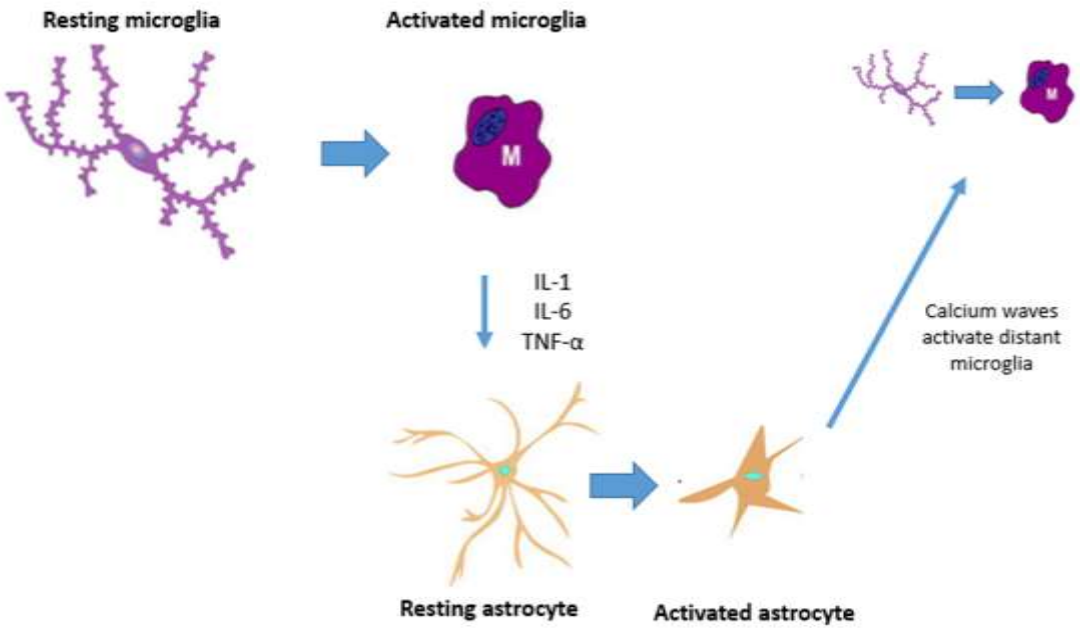

Figure 5-Schematic representation of microglia and astrocytes cross talk. *Following nerve injury, neuroinflammation is triggered at injury site leading to the infiltration of immune cells to the site of injury Microglia cells are activated at initial stages of pain progression and produce IL-1α and β, TNF-α, IL-6, between others, inducing astrocytes activation which is important to sustain pain sensation trough the time (Watson & Frank, 2013). Activated astrocytes prime to a calcium-wave, responsible for distant microglia activation, resulting in pain perception in regions distant from the original wound (Nedergaard & Dirnagl, 2005).*

3. Bladder function

3.1 Neuronal control of bladder function

The lower urinary tract (LUT), composed of a reservoir (the urinary bladder) and an outlet unit (the bladder neck, urethra and striated muscles of the external urethral sphincter), stores urine as it is produced and eliminates urine when bladder capacity is reached. Normal LUT function requires synchronization between bladder contraction and relaxation of the urethral sphincter and depends on the coordinated activity of neuronal circuits involving peripheral and centrally located neurons. Control of the lower urinary tract (LUT) is a complex and multilevel process, which involves both peripheral and central structures (Fowler et al., 2008).

Urine is constantly produced and accumulated in the urinary bladder. Urine storage produces low intensity firing of bladder sensory afferents, which stimulates sympathetic input to the bladder outlet (bladder base and urethra) and to the external urethral sphincter resulting in continuous contraction of the bladder outlet and relaxation of the detrusor muscle (Fowler et al., 2008). Once enough urine is accumulated in the bladder, wall stretch activates sensory afferents. Fullness sensation is conveyed to the lumbosacral spinal cord where ascending neurons transmit this information to the periaqueductal grey area (PAG) and, from there, to the cerebral cortex. The individual becomes aware of how full your bladder is and makes a decision of going to the toilet or postponing micturition. If the decision is to void, PAG neurons will transmit that information to the pontine micturition center, located in the brainstem (Fowler et al., 2008). Information will then be relayed to spinal motoneurons. The sympathetic tone of the bladder will be interrupted, promoting opening of the bladder neck and stopping detrusor relaxation. Spinal motoneurons of the Onuf's nuclei become inhibited, further relaxing the urethral sphincter and local parasympathetic bladder innervation becomes active and stimulates detrusor contraction. As a final result, the detrusor contracts, the urethra relaxes and urine will be removed (Figure 6).

This sequence of events highlights a series of important facts: 1) the lower urinary tract (LUT; composed by the urinary bladder, the bladder neck, urethra and striated muscles of the external urethral sphincter), alternates between urine storage and its elimination; 2) a strict coordination between the reservoir and the outlet is required for proper LUT function; 3) LUT control is regulated by complex circuits involving various neurons located at the central (CNS) and peripheral nervous system; 4) LUT function is under voluntary, learned control developed during maturation of the CNS. The considerable complexity of neuronal mechanisms regulating LUT function renders it highly sensitive to a variety of injuries and diseases, particularly those affecting the CNS such as MS.

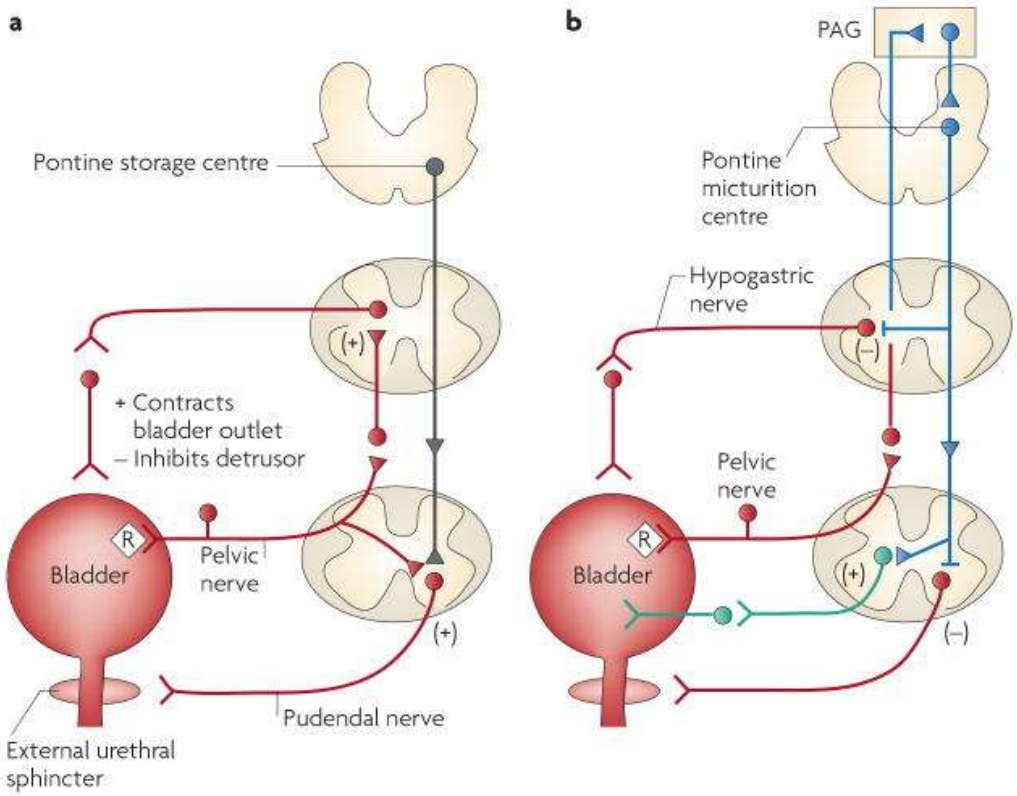

Figure 6-Neural circuits that control storage and urine voiding. *A. Urine storage reflexes: When the bladder is empty sympathetic firing inhibits contraction of detrusor and sympathetic outflow is stimulated in the bladder, urethra and in the external urethral sphincter is stimulated. B. Voiding reflexes: As the bladder fill, the pressure inside enhance and leads to intense bladder-afferent firing which activate spinobulbospinal reflex pathways (blue) that pass through the PMC. The parasympathetic outflow to the bladder and urethral smooth muscle is stimulated (green) and sympathetic and pudendal outflow to the ureteral outlet (Jardin et al.) is inhibited.*

3.2 Bladder dysfunction in Multiple sclerosis

Lower urinary tract dysfunction (LUTD) results from impairment of neurotransmission within the CNS, reflecting demyelination and axonal degeneration occurring not only at the spinal cord level but also in the brain. Approximately 90% of all MS patients will develop LUTD at some point of disease progression (Aharony et al., 2017), including detrusor overactivity (DO), detrusor hypocontractility, and/ or detrusor- sphincter dyssynergia (Panicker & Fowler, 2015). At least 50% of patients with no urinary complaints present urodynamic abnormalities, indicating that the real prevalence of bladder dysfunction in MS patients is underestimated (Fowler et al., 2009). The most common bladder symptoms, reported by patients, are frequency, urgency,

incontinence and, less frequently, obstructive symptoms (de Seze et al., 2007). Hesitancy in starting micturition, and inability to empty the bladder completely, can also occur.

For MS patients, bladder problems not only seriously compromise the quality of life but may also lead to LUT infections and deterioration of the upper urinary tract (Caramella et al., 2011). Thus, treatment aims to improve the quality of life by reducing incontinence and ameliorating storage symptoms and bladder emptying, while avoiding urological complication, such as urinary tract infections, bladder and kidney stones, hydronephrosis, and renal function deterioration. (Aharony et al., 2017). Depending on disability of patient, cognitive function, manual dexterity, mobility, amount of economic possibilities and support at home, a specific treatment program is selected to deal with bladder dysfunction. Treatment may be initiated by bladder training, useful and effective in patients with mild disability (Amaro et al., 2005). Antimuscarinic drugs, alone or in combination with intermittent catheterization, are currently the first line medical treatment in impaired storage situation. If patients are refractory to antimuscarinics, botulinum neurotoxin type A (BoNT/A) is also used, as it is now the gold-standard treatment for neurogenic DO (Cruz et al., 2011; Ginsberg et al., 2013). Other therapeutic options include neuromodulation, intermittent catheterization (IC), and indwelling urinary drainage.

II. Research goals

II. Research goals

A recent study showed that knockout mice for Transient Potential Receptor Vanilloid 1 (TRPV1) were protected from MS, presenting delayed disease onset, reduced clinical scores and reduced demyelination. Protection conferred by TRPV1 absence seemed to relate to diminished BBB permeability, preventing inflammatory cell extravasation into the CNS and consequent myelin degradation (Paltser et al., 2013). TRPV1 is an ion channel expressed by small-to-medium diameter sensory neurons (Avelino et al., 2013; Mickle et al., 2015).

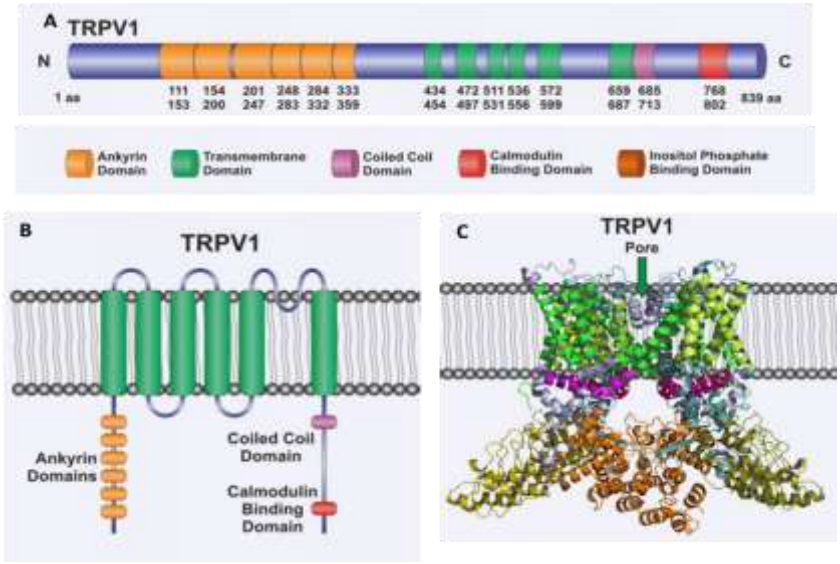

Figure 7- Molecular structure of TRPV1. *(A) scheme of TRPV1 channel depicting individual domains. Numbers correspond to amino acid positions of human TRPV1. (B) Representation of TRPV1 monomers morphology. The pore is localized between transmembrane domains 5 and 6, and both N-terminal and C-terminal domains localized in the cytosol. (C) Representation of the frontal view of the channel. Adapted from (Jardin et al., 2017)*

It is also present in nerve fibres coursing in the skin and urinary bladder, where it can also be found in urothelial cells (Avelino et al., 2013; Charrua et al., 2009). TRPV1 is also present in airways (Szallasi et al., 1993), urethra (Parlani et al., 1993) nasal mucosa (Rinder et al., 1996) colon (Goso et al., 1993) and in several brain nuclei (Mezey et al., 2000). The structure of TRPV1 follows the pattern of the TRP channels, with six transmembrane spanning domains, six ankyrin

repeats in the N-terminus and a large C-terminal region (Cao et al., 2013) (Figure. 7).TRPV1 is involved in the regulation of body temperature (Alawi et al., 2015) and its activation leads to painful, itching and burning sensations (Caterina et al., 2000). This receptor can be activated by a wide variety of exogenous and endogenous physical and chemical stimuli. The classical exogenous activators of TRPV1 include vanilloid substances, as capsaicin, noxious heat (>43°C) (Caterina et al., 1997), low pH (Jordt et al., 2000), resiniferotoxin (RTX), a potent capsaicin analogue (Alawi & Keeble, 2010) and other natural and synthetic hydrophobic TRPV1 agonists (Geron et al., 2017). Endogenous TRPV1 agonists include N-arachidonyl-ethanolamine, lipoxygenase compounds, N-acyldopamines and other long-chain unsaturated fatty acid such as endocannabinoid and endovaniloids (Huang et al., 2002) (Yin et al., 2013; Ryan & Gibson, 2014).

Several animal models and clinical studies show that TRPV1 expression and activity are upregulated in chronic pain conditions and urinary dysfunction. Blockade of this receptor with specific antagonists or its long-lasting desensitization by peripheral administration of potent agonists has been shown to reduce pain (Ghilardi et al., 2005; Moran et al., 2011; Szallasi et al., 2007; Szallasi et al., 2006; Walker et al., 2003) and improve urinary dysfunction (Birder, 2007; Cruz et al., 1997; Gunthorpe and Szallasi, 2008; Silva et al., 2000; Silva et al., 2005). It is presently unclear if TRPV1 is involved in pain and bladder dysfunction in MS, a matter we aimed to investigate in the present study.

Specifically this study had two main goals:

- **To establish an characterize a model of EAE in terms of pain development and bladder reflex activity and identify behavioral signs of disease progression**

For that, rats were immunized (see in materials and methods section) and monitored for 38 days, during which cutaneous sensitivity and bladder function were assessed by a series of behavioral tests.

- **To test if TRPV1 desensitization could alleviate pain and improve bladder function in rats with established EAE**

For that, EAE rats received intrathecal RTX and cutaneous sensitivity assessed. At the end, animals were submitted to cystometries under urethane anesthesia to assess bladder reflex activity.

III. Materials and methods

III. Material and Methods

1. Animals

Experiments were performed in 250-300 g female Wistar rats (obtained from the vivarium of the Faculty of Medicine of Porto, derived from the Charles River strain, France). All animals were housed under controlled conditions of light (12h light/12h dark schedule), temperature (20-24°C) and humidity (55% +/- 10%), with free access to food and water. Experimental procedures were carried out according to the European Communities Council Directive 2010/63/EU, to ethical guidelines for investigation of pain in animals (Zimmermann, 1983) and internal regulations of the Faculty of Medicine of Porto. All efforts were done to reduce the number of animals used and their suffering.

2. Reagent and drugs

EAE induction and intrathecal RTX injections were performed under isofluorane anaesthesia (IsoFlo; Abbott Laboratories, Maidenhead, UK). Cyclosporine (SIGMA-Aldrich, USA, 4mg/Kg) was dissolved in sterile saline and injected subcutaneously. Complete Freud's Adjuvant (CFA), resulting from Mycobacterium butyricum (Difco Laboratory, USA), diluted in paraffin oil (Confar, PT), saline, tween 80 (Sigma, Germany) together and myelin protein (MBP; Sigma, Portugal, ref.1861) were necessary for EAE induction. For intrathecal RTX administration a stock RTX solution (10 µM) was used. The respective vehicle solution was 10% ethanol in sterile saline. For terminal handling and cystometries, animals received a subcutaneous injection of urethane (1.2 g/kg), and a saline solution (NaCl 0.9%) was infused through the bladder. Primary and secondary antibodies used in immunohistochemistry reactions are listed in tables bellow (Table 1 and 2).

Table 1-**Primary antibodies description.**

Primary antibodies	***Target/Specification***	***Dilution***	***Host***	***Manufacturer***
	MBP	1:1000	Rabbit	Abcam
	Iba-1	1:1000	Rabbit	Wako
	GFAP	1:2000	Mouse	CellSignaling
	ATF3	1:300	Rabbit	SantaCruzBiothecnology
	CGRP	1:8000	Mouse	Abcam
	IB4	1:1000	Rabbit	SIGMA-Aldrich
	TRPV1	1:1000	Mouse	SantaCruzBiothecnology
	C-Fos	1:5000	Rabbit	CalbioChem

Table 2- **Secondary antibodies and secondary detection reagents description.**

Secondary antibodies	***Target/specification***	***Dilution***	***Host***	***Manufacturer***
	Rabbit/Alexa 568	1:1000	Goat	Molecular Probes Europe
	Rabbit/Alexa 488	1:1000	Goat	Molecular Probes Europe
	Mouse/Alexa 488	1:1000	Goat	Molecular Probes Europe
	Mouse/Alexa 568	1:1000	Goat	Molecular Probes Europe
	Polyclonal anti-Rabbit Biotinilated	1:200	Swine	Dako Denmark
	Streptavidin Alexa™ fluor 488 conjugate	1:1000	mouse	ThermoFisher

.

3. Induction of Experimental Auto-immuno Encephalitis (EAE)

The model of MS chosen in the present study was the classical Experimental Auto-immuno Encephalitis (EAE) modified by Thibault and coworkers (Thibault et al., 2011). Briefly, under isofluorane anaesthesia (5% for induction, 2% for maintenance), rats received a single subcutaneous injection in the flank of 100µl of a suspension made of: 1 ml CFA containing 4 mg of Mycobacterium butyricum and 500 µg of bovine MBP dissolved in 0.1 ml of saline. After EAE induction, from the day of EAE induction until the end of the experimental period, animals received a subcutaneous injection of Cyclosporine A (4 mg/kg) three times a week.

4. Behavioural studies

All animals were subjected to a two weeks habituation period before EAE induction of the EAE to avoid stress reactions due to manipulation and placement in the testing arenas. During the first week, animals were habituated to handling and hind back skin probing (necessary for subsequent subcutaneous cyclosporine administration). During the second week, animals were habituated to the different behavioural tests to determine the mechanical and thermal (hot and cold) thresholds. The basal thresholds were determine one week prior to EAE induction, after which mechanical sensitivity was assessed on specific days during disease progression.

Mechanical sensitivity was assessed using the von Frey test, which was applied twice a week. The mechanical thresholds (MTs) were established with the Von Frey monofilaments using the up-down method. Rats were placed in individual chambers (23 x 17 x 14 cm) with a wire mesh floor and allowed to acclimate for 15 minutes or until cage exploration stopped. A punctate stimulus was applied to the mid-plantar area of the left hind paw with one of a series of eight Von Frey monofilaments (rated at 1, 1.4, 2, 4, 6, 8, 10, 15, 26, 60, 100 g). Filaments were applied 5 seconds perpendicularly with enough strength to cause the monofilament to slightly bend. Testing was initiated with the 1 g monofilament. The remaining filaments were applied in a consecutive fashion. In case of no response to the filament, the next-stronger monofilament was applied. A positive response was recorded when the rat reacted to the filament (suddenly lift the paw or jump) and do not react to the previous one.

Thermal sensitivity to hot and cold temperatures at hindpaws was assessed with the hot/cold plate (Bioseb, Chaville, France). For that, animals were placed in a transparent plastic box (22x28). Five minutes after placement or after cage exploration stopped, the temperature of de plate was increased from 32°C to 52°C (heat sensitivity) or decreased from 22°C to 0° C (cold sensitivity). In both cases, the temperature changed in a similar rate (5ºC/min). The temperature, in the hot or cold range, at which the animal showed the following behaviours was recorded (Thibault et al., 2011):

Awareness: The animals stopped exploring or grooming and turned his head towards his hind paws. This behaviour was observed for temperatures between 16-18°C for cold temperatures and between 36-40°C for hot temperatures, in both control and EAE animals before disease induction and was interpreted as an awareness of changes in cold or heat perception.

Discomfort: The animal stopped moving and started placing his body weight on his toes, rather than on the full surface of his hind paws. This behaviour was considered as signal of discomfort but not yet a painful response. This was observed in control and EAE animals before disease induction at 12-16 °C for cold temperatures and between 43-46 °C in case of hot temperatures.

Nociception: The animal exhibits one of the following: withdrawing, licking or shacking one of his hind paws or jumping. This behaviour was noticed at 0-3°C for cold temperatures and in case of hot temperatures at 46-50 °C in control and EAE animals before disease induction.

5. Cystometries

Six weeks after EAE induction, animals was deeply anaesthetized with a subcutaneous injection of urethane (1.2 g/kg) and submitted to cystometries to fully characterized bladder activity. When deeply anaesthetized, the bladder was exposed through a small, low abdominal incision. A 21-Gauge needle was inserted in the bladder dome. Animals were left untouched for 15-30 min to allow bladder stabilization, after which saline infusion was initiated (constant rate of 6ml/h), while bladder reflex activity was recorded for 1 hour. Body temperature was maintained at 37°C with a heating plate. The cystometrograms obtained were analyzed using LabScribe2 software (iWorx, World Precision Instruments).

6. Intrathecal RTX administration

Intrathecal RTX delivery was performed according to a protocol adapted from Ossipov et al (Ossipov et al., 1988) and De la Calle et al (De la Calle & Paino, 2002; Adaes et al., 2017). For that, EAE animals were anaesthetized with isofluorane (5% for induction, 2% for maintenance) and lumbar dorsal area was shaved and the skin was swabbed 70 % alcohol. The abdomen-pelvic region was lifted to create a slight curvature in the vertebral column at vertebral level L5-S1, which was localized using the anterior part of the iliac crest as a tactile reference point for the L6 vertebra. The rats were then gripped firmly by the hip bones with one hand while with the other hand the L5-6 and the L6-S1 intervertebral spaces were identified using the index finger. Animals were injected with 100 µL of RTX (0,1 µg/kg) (Cruz et al., 2008a) or vehicle solution (10% ethanol in sterile saline) at the L5-L6 intervertebral space with a 21 G insulin syringe by introducing the needle through the widest intervertebral space, lowering it until contact with the vertebral body and penetrating into the intrathecal space (perceived by a change of resistance). Correct dura puncture and position of the needle tip was verified by a reflexive flick of the tail or a hindpaw flinch.

7. Perfusion and immunohistochemistry

After all cystometries, animal were perfused and fixed and the spinal cord, dorsal root ganglia (DRG) and left sciatic nerves were collected. Animals were perfused through the ascending aorta with 250 mL of calcium-free Tyrode's solution (0.12 M NaCl, 5.4 mM KCl, 1.6 mM $MgCl2•H2O$, 0.4 mM $MgSO4•H2O$, 1.2 mM $NaH2PO4•H2O$, 5.5 mM glucose and 26.2 mM $NaHCO3$) followed by 4% paraformaldehyde (PFA) in 0.1 M phosphate buffer (PB). All tissue collected was post-fixed for 5h in 4% PFA and cryoprotected overnight in 30% sucrose in PB with 0.1% sodium azide. Transverse serial spinal cord (20 µm-thick) sections and longitudinal serial 12 µm-thick DRG

sections were obtained in a LEICA cryostat, collected in Superfrost Plus slides and stored at -20°C until further processing.

For immunofluorescence analysis, alternate slides of spinal cord, DRG and sciatic nerve thawed and thoroughly washed in with 0.1 M phosphate buffer saline (PBS) and PBS containing 0.3% Triton X-100 (PBST) and blocked with 10% of normal goat serum (Franken et al.) in PBST for 1 hour. Sections were then incubated for 48h at 4oC in primary antibodies solutions diluted in 2% NHS in PBST (for spinal cord sections: anti-MBP 1:1000; anti-Iba-1 1:1000; anti-GFAP 1:200; anti-CGRP 1:8000; anti-Ib4 1:1000; for dorsal root ganglia (DRG): anti-ATF3 1:300. After several washes with PBST, sections were incubated with species-specific Alexa™ flurochrome-labelled antibodies or Alexa™ flurochrome-labelled streptavidin for 1h at room temperature. Immunostainings were controlled by omitting the primary antibody. After washes with PBST and PBS, sections were mounted with Prolong Gold© mounting medium (Molecular Probes©, USA) and representative images were obtained in a Zeiss microscope (Axioimager Z1, Zeiss, Germany) using the Axiovision 4.8 software.

Detection of c-Fos immunoreactivity in spinal cord was performed using the ABC method. Briefly, sections were thoroughly washed in PBS. After inhibition of endogenous peroxidase activity and further washes in PBS and PBST, sections were incubated in 10% normal swine serum in PBST for 2 h. Sections were then incubated for 48 h at 4 ºC with a specific antibody against c-Fos (1:5000). Subsequently, sections were washed in PBST and incubated for 1 h with polyclonal swine anti-rabbit biotin conjugated antibody (1:200; Dakopatts, Denmark). In order to visualize the immunoreactions, the ABC conjugated with peroxidase (1:200; Vector Laboratories, UK) method was used with 3, 3 diaminobenzidine-tetrahydrochloride as chromogen (DAB; 5 minutes in 0.05 M Tris buffer, pH 7.4 containing 0.05 % DAB and 0.003 % hydrogen peroxide). Sections were mounted on gelatine-coated slices and air-dried for 12 h, cleared in xylene, mounted with Eukitt mounting medium and cover-slipped.

8. Quantification and Statistics

All statistical analyses were conducted using SigmaStat 3.11 or GraphPad softwares. Behavior results were analyzed by Friedman Repeated Measures Analysis of Variance on Ranks, which was followed by the post-hoc test Student-Newman-Keuls. Cystometograms were analysed using the LabScribe software (version 2.34900; iWorx Systems). Results from intensity labeling, number of cells and behavioral results from pre- and post- RTX injection data sets that proved not to be normally distributed (Shapiro-Wilk normality test), was analyzed by a non-parametric Mann-Whitney test. The data sets that followed a normal distribution was analyzed by a t-test. For analysis of immunofluorescence intensity and glial cell counting, images were digitally acquired under fixed parameters. Five non-contiguous spinal cord sections were photographed per animal to further analyze with imageJ software. MBP, GFAP, CGRP, TRPV1 and MBP expression as well as IB4 binding were quantified by densitometry using image J. To count activated microglial active cells, labelled with iba-1, we considered cells with globular form with short or none processes. The number of c-Fos immunoreactive (IR)-cells was counted in the dorsal horns (Avelino et al., 1999) dorsal commissure (DCM) and intermediolateral grey matter areas of the cord (ILGs). Data is represented as mean ± standard deviation (SD). In all cases, $p < 0.05$ was considered statistically significant. Data is presented as the mean ± SD.

IV. Results

IV. Results

1. EAE model induction, validation and characterization

1.1 Behaviour analysis

1.1.1 Cutaneous sensitivity to mechanical stimuli

Before EAE induction, the hindpaw mechanical threshold (MT) of EAE animals was 42.7±26.9g, similar to that observed in control animals 26.2±18.8g (Figure 8).

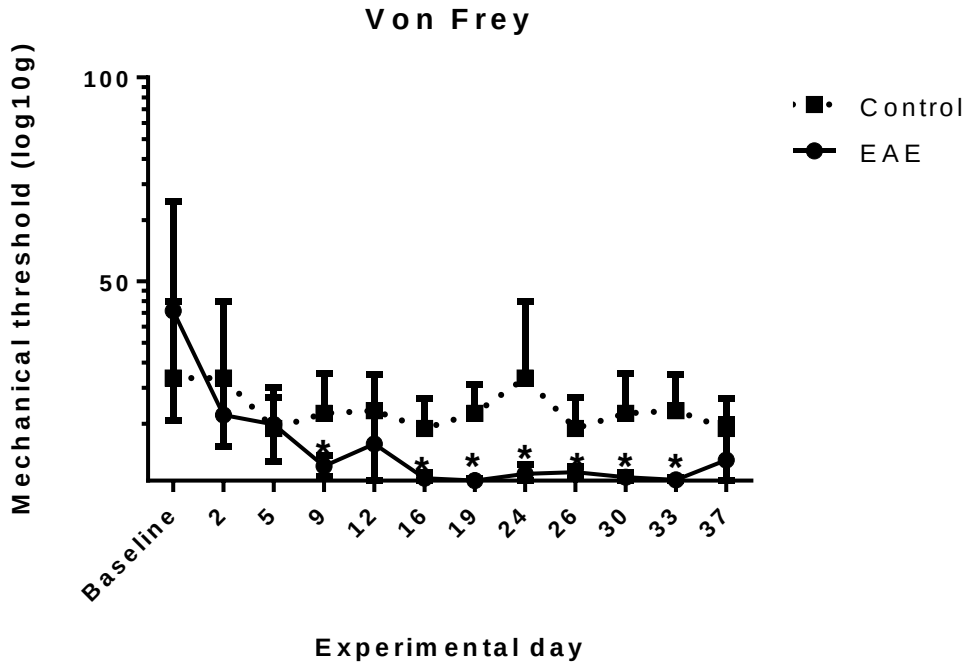

Figure 8- Time course of changes in cutaneous sensitivity to mechanical stimulation of the left hindpaw of control and EAE rats. *While the mechanical threshold (MT) remained at constant values throughout the experimental period (37 days) in control animals, it significantly decreased on experimental day (ED) 9 and from ED16 to ED 33. Results are presented as mean ± SD (n=6 per experimental group). Two way ANOVA, not repeated measures, followed by a post-hoc t-test. 'EAE vs control' *p < 0.001. Post-hoc t-test indicate statistically significant differences at the time points indicated. 'ED9' *p= 0.0116; 'ED16' *p= 0.0026; 'ED19' *p= 0.0002; 'ED30' *p= 0.003; 'ED33' *p=0.0009.*

While the MT remained at similar values in control animals during the experimental period, it started decreased from experimental day (ED) 9 onwards, when it decreased to 4.6±2.6 ($p<0.05$ versus control animals), suggesting development of mechanical allodynia in EAE rats (Figure 1). The MT reached its lowest value on ED33 (1.17±0.5 $p<0.05$ versus control) (Figure 1). At two time points, ED12 and ED33, the MT increased to 10±9.1 and decreased to 1.17±0.5, respectively, indicating some fluctuation in cutaneous sensitivity.

1.1.2 Cutaneous sensitivity to thermal stimuli in the heat range

Slight variations were found in control and EAE groups in regard to awareness and nociceptive behaviours in the hot-plate test. Control animals reacted at 35.0±0.493 °C (awareness) and 46.2±0.416 °C (nociception) at baseline and did not present significant differences until the end of experimental time (ED38), when values recorded were 38.8±2.48 °C (awareness; Figure 9A) and 46.4±0.79 °C (nociception; Figure 9C). In EAE animals the temperature at which the animals reacted before disease induction were 41.9±14.7 °C (awareness) and 50.7±0.7 °C (nociception). At the end of experimental period, temperatures of reaction in EAE animals were 38.8±1.86 °C (awareness; Figure 9A) and 46.4±3.0°C (nociception; Figure 9C). At ED31, significant differences were found between controls (38±0.86 °C) and EAE (40.5±3°C) in regard to awareness heat reaction(Figure 9A).

In what concerns discomfort (Figure 9B) reactions to heat stimulation, control animals reacted to similar temperatures throughout the experimental period, values being 38.3±2.67°C, at baseline and 44.2± 0.99°C, on ED38. In what concerns EAE rats, an oscillatory response was observed from baseline to ED38. At ED10 the discomfort sensation in EAE had risen from baseline values (45.4±1.26°C) to 43.9±2.30°C. At ED17, the reaction temperature further decreased to 37.9±2.33°C and increased to 44.7±2.8°C at ED38. At ED31 a significant difference was found between control and EAE animals (*$p<0.05$).

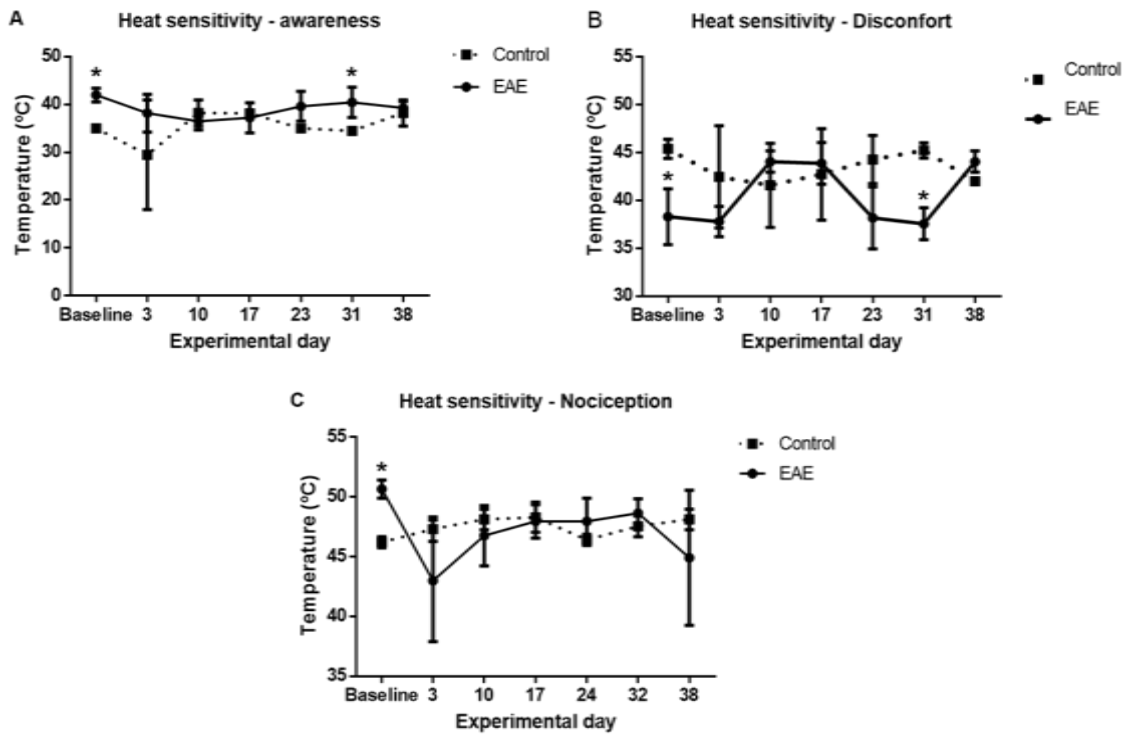

Figure 9 -Time courses of hot plate test. *Threshold of awareness, discomfort and nociception reactions due to temperature rise (From 32°CC to 52°C) at level of hindpaws in EAE and Control animals during the experimental time. In regard to awareness (A) and Nociception (C), temperatures were almost constant to controls and EAE (the last, represented by the continuous line). A significant difference was found to EAE at ED31 with a high awareness reaction. Related to discomfort an oscillation in temperature of reaction was found, with significant differences at ED31. Results are expressed as mean ± SD. Were included: n = 6 'EAE' 'and n = 6 'Control' in which graph. Statistical tests: Shapiro-Wilk normality test; Two way ANOVA, not repeated measures, followed by multiple tests to two away ANOVA. Both 'EAE' and 'Control' passed normality test (Alpha=0.05). Two way ANOVA: 'EAE - Awareness vs Control - Awareness' Post-hoc t-test indicate significantly differences at the time points indicated. 'Baseline' *p < 0, 0001; 'ED31' *p= 0, 00022. 'EAE - Discomfort vs Control – Discomfort 'Post-hoc t-test indicate significantly differences at the time points indicated. 'Baseline' *p < 0, 0001; 'ED31' *p= 0, 0003. 'EAE - Nociception vs Control - Nociception' Post-hoc t-test indicate significantly differences at the time points indicated. 'Baseline' *p < 0, 0001.*

1.1.3 Cutaneous sensitivity to thermal stimuli in the cold range

No statistically significant differences were found in sensitivity to cold between control and EAE animals.

Slight variations were found in control and EAE groups to awareness and discomfort in cold plate test. Control animals reacted at 18.9±0.78°C (awareness; Figure 10A) and 15.7±0.7°C (discomfort; Figure 10B) before disease induction. At the end of experimental period, temperatures of reaction in control animals were 18.4±1.22 °C (awareness) and 12.5±6.03°C (discomfort). In EAE animals temperatures of reaction were 15.3± 2.11 °C (Awareness) and

8.80±1.15 (discomfort) at baseline and did not present significant differences until the end of experimental time. (ED38) when values record were 19.8 + 1.17 (awareness) and 16.48+2.72 (discomfort).

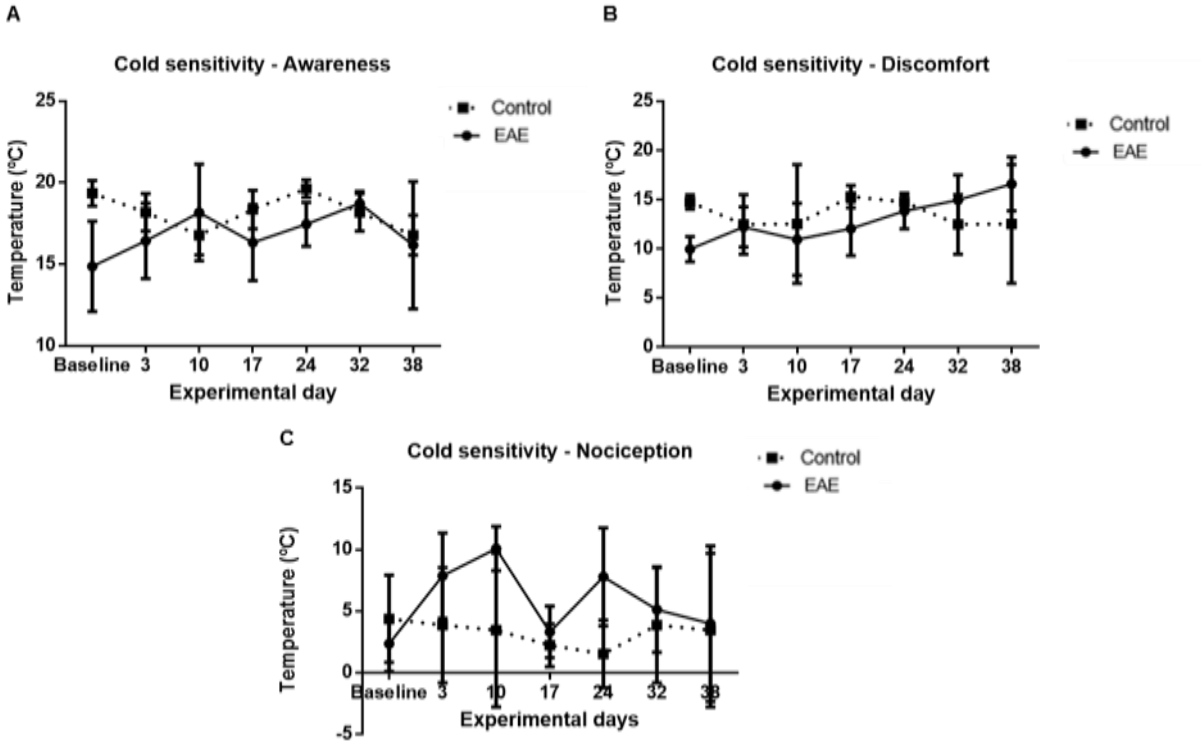

Figure 10-Time courses of Cold plate test. *Threshold of awareness, discomfort and nociception responses due to temperature decrease (From 22°C to 0°C) at the level of hindpaws in EAE and Control animals. No statistically significant differences were found in sensitivity to cold between control and EAE animals. Fluctuations during experimental time was observed at EAE group in regard to nociceptive response (C). Results are expressed as mean ± SD. Were included: n = 6 'EAE' 'and n = 6 'Control' in which graph. Statistical tests: Shapiro-Wilk normality test; Two way ANOVA, not repeated measures, followed by multiple tests to two away ANOVA. Both 'EAE' and 'Control' passed normality test (Alpha=0.05). Two way ANOVA: 'EAE - Awareness vs Control - Awareness'; EAE - Discomfort vs Control – Discomfort'; 'EAE - Nociception vs Control - Nociception': No significant differences was found for none of sensations.*

Still, while control animals reacted at similar temperatures throughout the experimental period (38 days) EAE show fluctuations in regard to cold nociception (Figure 10C). Control animals reacted to 3.75 ±4.27°C, at baseline and to 2.73 ± 1.60°C, at the end of experimental time. EAE animals at ED10 show nociceptive sensation rise from 2.35±1.71°C, at baseline to 10.08 ± 6.61°C. The reaction temperature further decrease to 3.32±2.39°C at ED17, and increase

to 7.78±1.6.26°C at ED24. Temperature of nociceptive reaction decrease again at ED38 to baseline closer values (3.98±3.31°C).

1.2 Bladder function

1.2.1 Paper filter results

In order to follow bladder function during the experimental period, a paper filter test was performed once a week. Analyses from paper filter test showed one or two spots per filter paper from controls and EAE animals at baseline. During the experimental period, only papers from EAE animals showed differences, with an increased number of urinary spots, which were smaller than at baseline.

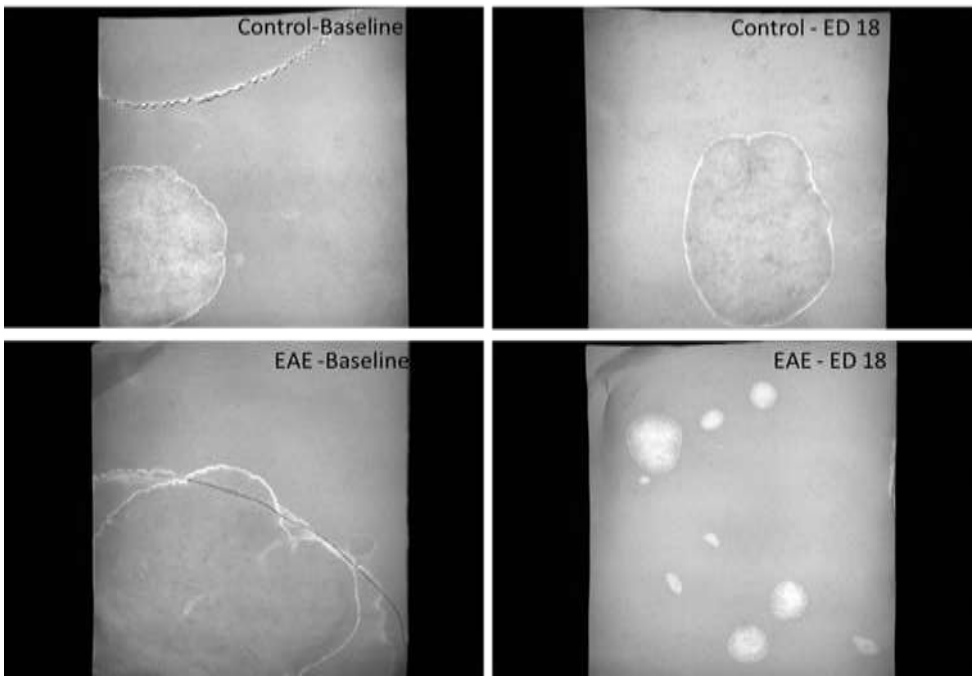

Figure 11- Images from paper filters collected upon urine test. *Controls maintained micturition pattern in filter paper during the experimental time. Contrarily EAE animals show high number of spots printed on paper from ED18 until the end of experimental time.*

1.2.2. Cystometries

At the end of experimental time (38 days) cystometries performed to evaluate the bladder function. In control animals, the frequency of bladder reflex contractions was 0.86 ± 0.27 and amplitude of 24.7 ± 3.7 cmH2O (Figures 12A, 13A; B). In EAE animals, the frequency of bladder contractions had significantly increased to 1.32 ± 0.86 and the amplitude was 15.27 ± 6.3 cmH2O (Figures 12B, 13A; B).

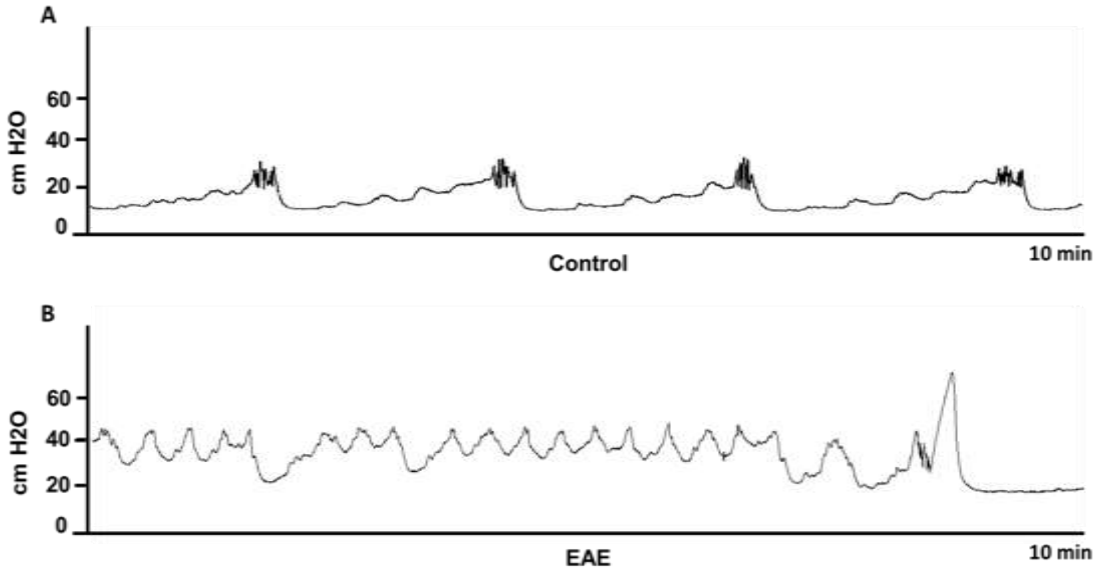

Figure 12- Representative cystometograms of control and EAE animals. *Control animals (A) has low number of bladder contractions, represented by each peak and the same bladder amplitude to each contraction (40 cmH_20). EAE animals (B) has a high number of bladder contractions presenting a fluctuation in the amplitude for each peak.*

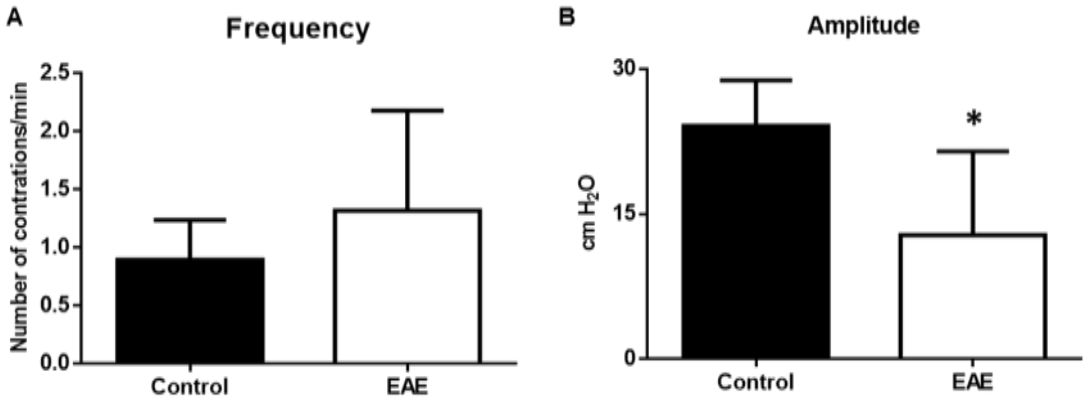

Figure 13-Histogram showing the mean frequency of bladder contraction and bladder amplitude. *EAE group has a higher number of contractions per minute than controls (A) and lower bladder amplitude (B).Results are expressed as mean ± SD. Were included: n = 6 control, n =6 EAE. Statistical tests: Shapiro-Wilk normality test, followed by Mann-Whitney test. Shapiro-Wilk test: Values don't follow a normal distribution. Mann-Whitney test: 'Control Frequency' versus the 'EAE frequency', don't significantly different; 'Control Amplitude' versus the 'EAE amplitude' group *p < 0.0001.*

1.3 Changes in neuronal tissue associated to EAE

1.3.1. MBP expression

To assess the degree of demyelination, immunostaining against MBP, a protein present in the myelin sheath, was performed. White matter labelling intensity was accessed by densitometry using imageJ. Myelin labeling was analyzed in the following areas: white matter adjacent to the dorsal (DHwm) and ventral (VHwm) horns and dorsal (DFwm) and ventral (VFwm) funiculus (Figure 14).

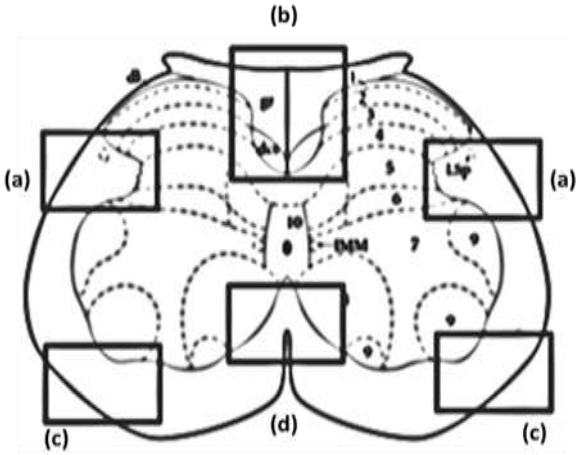

Figure 14- Schematic representation of the white matter analyzed areas by densitometry to MBP reaction. ***a)Dorsal horn adjacent white matter (DHwm); b) Dorsal funiculus white matter (DFwm); c) Ventral horn adjacent white matter (VHwm); d) Ventral funiculus (VFwm).***

Results (Figure 15 and 16) obtained show lower MBP intensity labelling in EAE animals (DHwm 56.57±18.22; VHwm 56.57±10.72; DFwm 38±19.32; VFwm 33.81±9.84) compared with control animals (DHwm 66.51±24.11; VHwm 57.61±21.00; DFwm 56.47±17.09; VFwm 59.30±24.22) at lumbar spinal cord (*p < 0.0001).

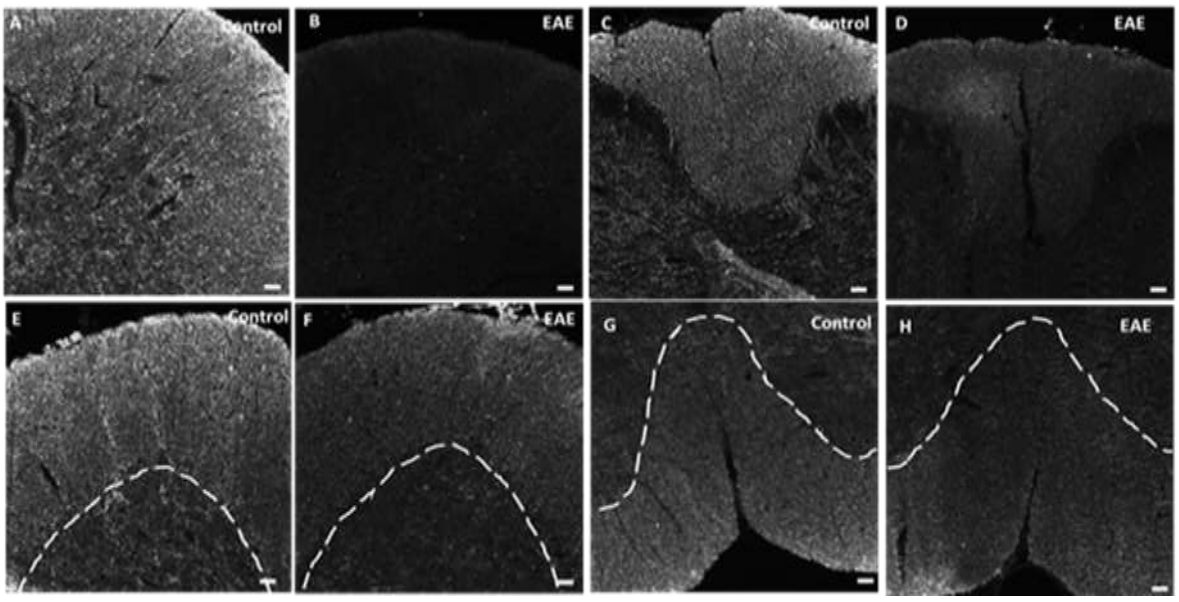

Figure 15- Expression of MBP at L5-S1 spinal cord sections*. A. Control dorsal horn adjacent white matter. B. EAE dorsal horn adjacent white matter. C. Control dorsal funiculus. D. EAE dorsal funiculus. E. Control*

ventral horn adjacent white matter. F. EAE ventral horn adjacent white matter. G. Control ventral Funiculus. H. EAE ventral funiculus. Scale bar 20 µm.

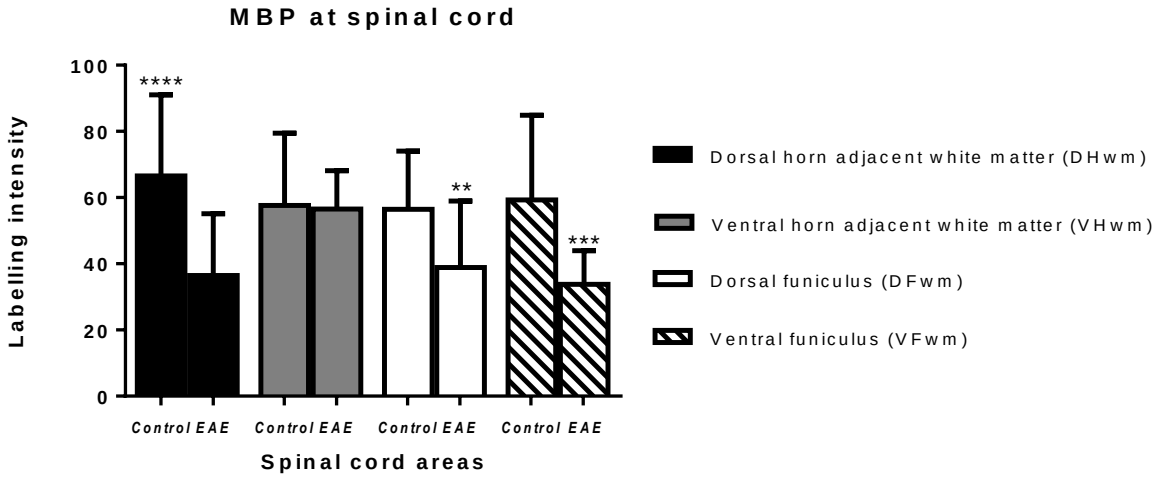

Figure 16- Mean of intensity labeling of MBP at L5-S1 spinal cord of Control and EAE animals. By the white matter analyzed areas a decrease in labeling intensity at white matter of lumbar spinal cord was observed in EAE group when compared to control animals. *Results are expressed as mean ± SD. Were included: n = 5 Controls; n = 5 EAE Statistical tests: Shapiro-Wilk normality test, followed by a t-student test. Shapiro-Wilk test alfa=0, 05; Student test: ' Control DHwm vs EAE DHwm' *P < 0.0001; ' Control VHwm vs EAE VHwm' not significantly different; ' Control DFwm vs EAE DFwm' *P < 0.05; ' Control VFm vs EAE VFwm' *P < 0.05; ' Control white matter vs EAE white matter' *P < 0.0001.*

To confirm if myelin loss was restricted to the CNS, expression of MBP was also assessed in sections from the left sciatic nerve. Although no quantifications were performed we found that MBP immunohistochemistry labelling was similar between control and EAE animals, indicating that demyelination was restricted to the CNS (Figure 17).

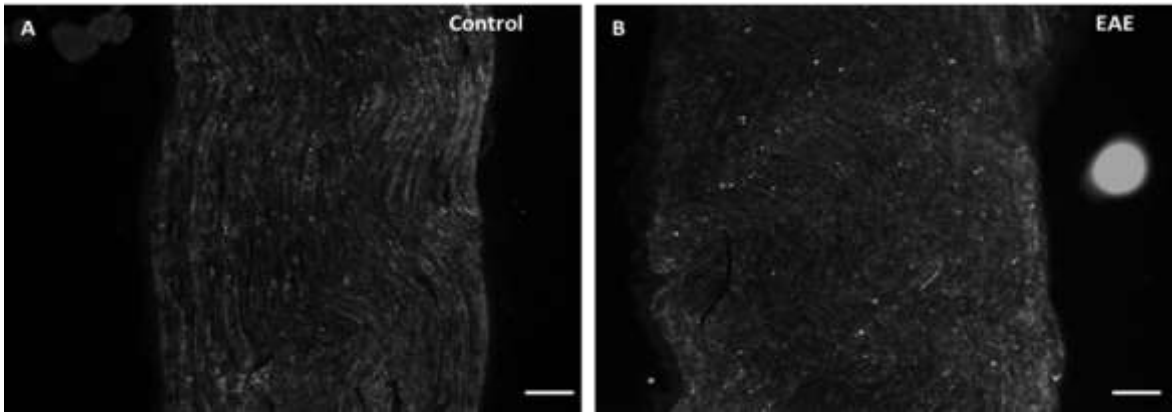

Figure 17- Expression of MBP *at sciatic nerve. EAE sciatic nerve MBP labelling (A). Control sciatic nerve MBP labelling (B). No differences was observed between the two groups. Scale bar 20 µm.*

1.3.2. ATF-3 expression at dorsal root ganglion

In addition, to exclude the possibility of peripheral injury due to EAE induction, the expression of ATF3, a marker of neuronal injury when present in the nucleus of DRG neurons (Adaes et al., 2015), was evaluated by immunohistochemistry. No immunoreactive nuclei were found in sections from control and EAE animals (Figure.18)

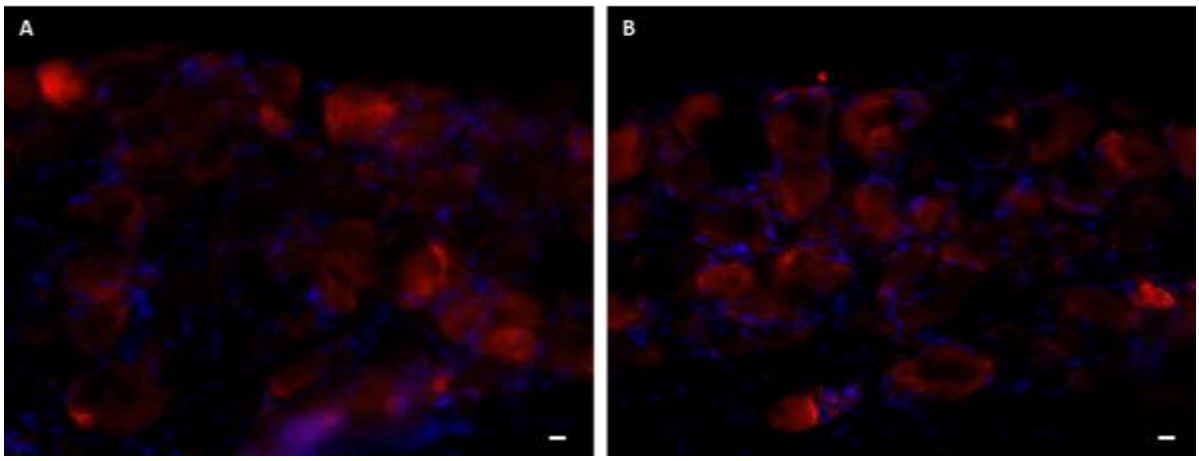

Figure 18- Expression of ATF-3 at L5 DRG*. No differences were found between controls (A) and EAE groups (B). Scale bar, 100 µm.*

1.3.3 Microglia at spinal cord level

An antibody against Iba-1 was used to label microglial cells at lumbar spinal cord (L5-S1). Labelling at superficial laminas (LI-LII) was less intense in control animals (43.8±33.7 in the dorsal horn) and 23.4±6.8 in the ventral horn; Figure 22) and microglia presented long processes and small and less globular body (Figures 19A and 20A). In contrast, labelling was more intense in sections from EAE animals (66.3±17.9 in the dorsal horn and 40.4±15.0 in the ventral horn; Figure 21) Cell shape had also changed and microglia presented shorter cellular extensions and globular body, indicating microglial activation (Figures 19B and 20B). Activated cells were counted in the dorsal and ventral horns. Very few activated microglial cells were found in sections from control animals (dorsal horn: 2.33±1.92, ventral horn: 1.11±1.54; Figure 21). The

number of activated cells was significantly increased in sections from EAE rats (dorsal horn: 22.2±11.5, ventral horn: 8.20±1.64; Figure 21).

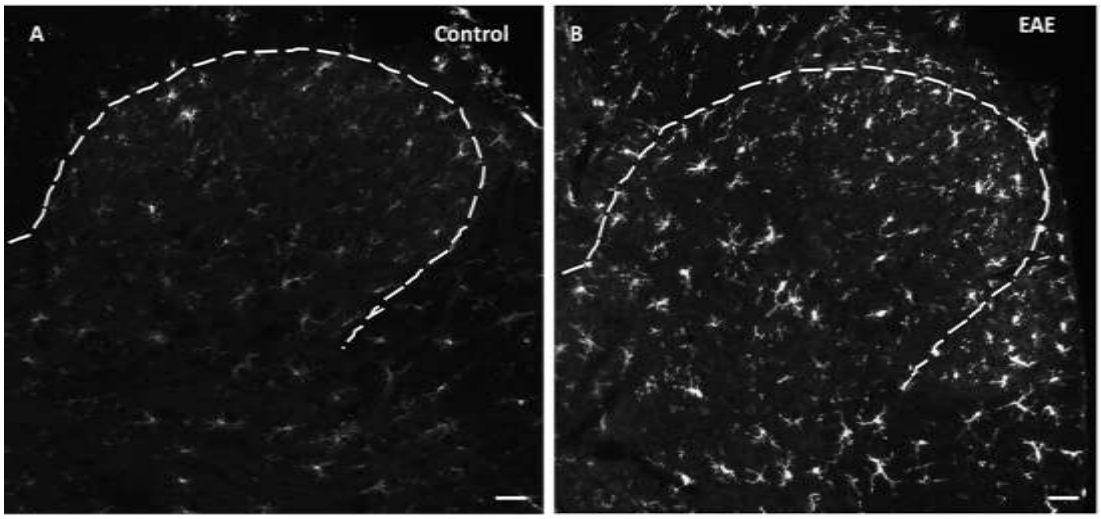

Figure 19- Expression of Iba-1 at dorsal horn of lumbar spinal cord. *Comparison between control and EAE animals. A significant enhance in the number of microglial cells in EAE animals can be observed. In addition, also in EAE animals, iba-1 labeled cells appear with a globular form and shorter processes, with a higher labelling intensity. Scale bar 20 µm.*

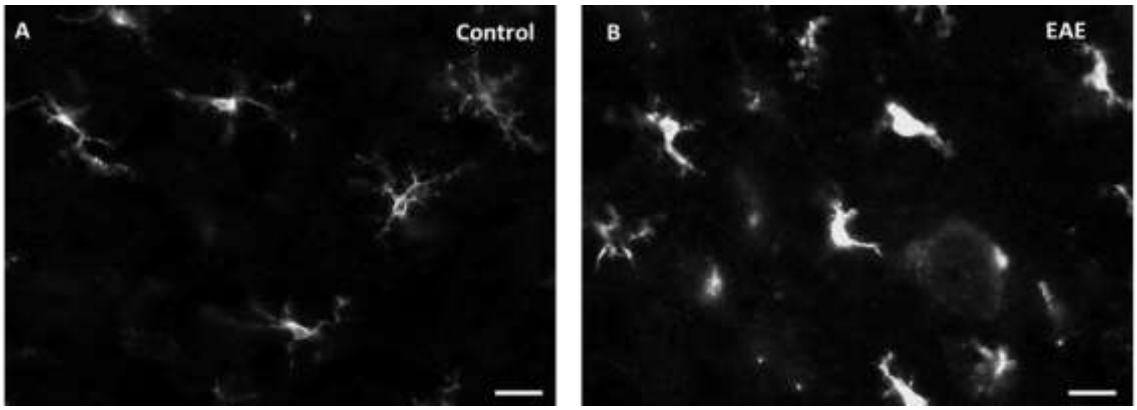

Figure 20- Morphology of cells labeled with Iba-1 antibody at dorsal horn of lumbar spinal cord. *Comparison between control (A) and EAE animals (B). Control animals (A) come up with a smaller cell body and thick and long processes. Animals with model induction (B) show higher intensity labeling, globular cells bodies with shorter or none processes. Scale bar 20 µm.*

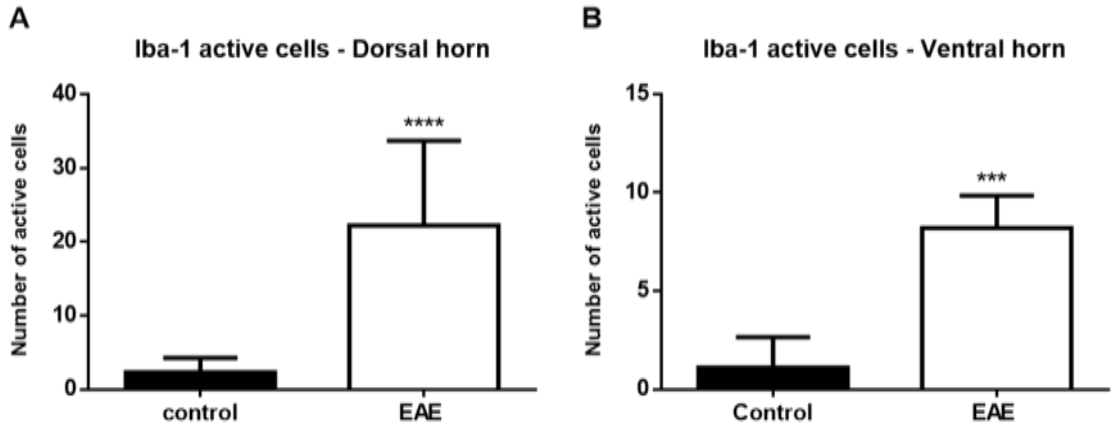

Figure 21- Number of Iba-1 activated at dorsal and ventral horns at L5-S1 spinal cord level*. EAE animals show a higher number of activated Iba-1 cells, with globular cell body and less or none processes in dorsal (A) and ventral horns (B). Results are expressed as mean ± SD. Were included: n = 3 Controls; n = 3 EAE Statistical tests: Shapiro-Wilk normality test, followed by a Mann-Whitney or t-test. Shapiro-Wilk test: Data sets from dorsal horn follow a normal distribution; Data sets from ventral horn do not follow a normal distribution; t-test: 'number of Iba-1 cells at dorsal horn from controls vs 'number of Iba-1 cells at dorsal horn from EAE ' ***P = 0.0001. Mann Whitney test: 'number of Iba-1 cells at ventral horn from controls vs 'number of Iba-1 cells at ventral horn from EAE '***P = 0.0001.*

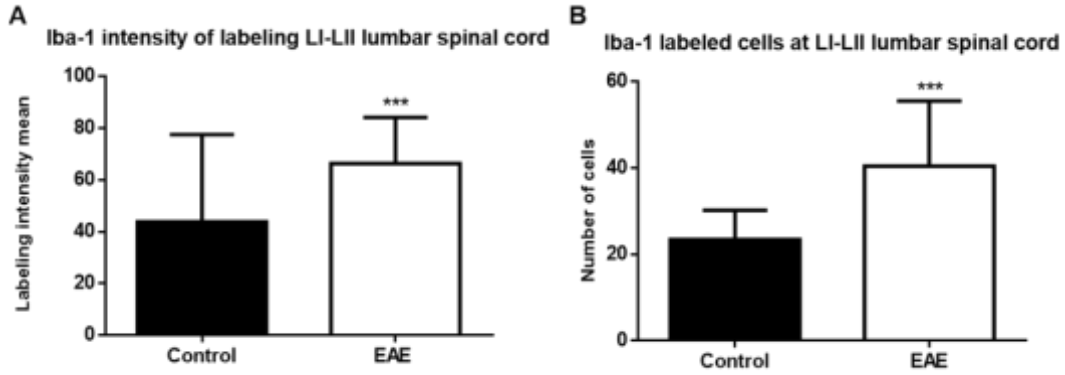

Figure 22- Intensity and total number of Iba-1 cells at superficial laminas of lumbar spinal cord (LI-LII). *Intensity (A) and number of cells (B) are both significantly increased in animals EAE inducted in comparison with control animals. Results are expressed as mean ± SD. Were included: n = 3 Controls; n = 3 EAE Statistical tests: shapiro-wilk normality test, followed by a Mann-Whitney test. Shapiro-Wilk test: Data sets do not follow a normal distribution; Mann Whitney test: 'Labeling intensity mean Control vs Labeling intensity mean EAE' ***P = 0.0001; 'Number of cells Control vs Number of cells EAE' ****p<0.0001.*

1.3.4. Astrocytes immunohistochemistry reaction at spinal cord level

To assess the astrocytic population at the lumbar spinal cord, GFAP immunohistochemistry labelling was performed. In control animals, astrocytes seem to present long and thin processes. In contrast, processes were shorter and the cell bodies seemed more condensed in sections from EAE rats. Although this morphology was also observed in white and gray matter, due to time constraints, the intensity of immunohistochemistry labeling was only quantified at ependymal canal (Figure.23) and no significant differences were found between the two animal groups.

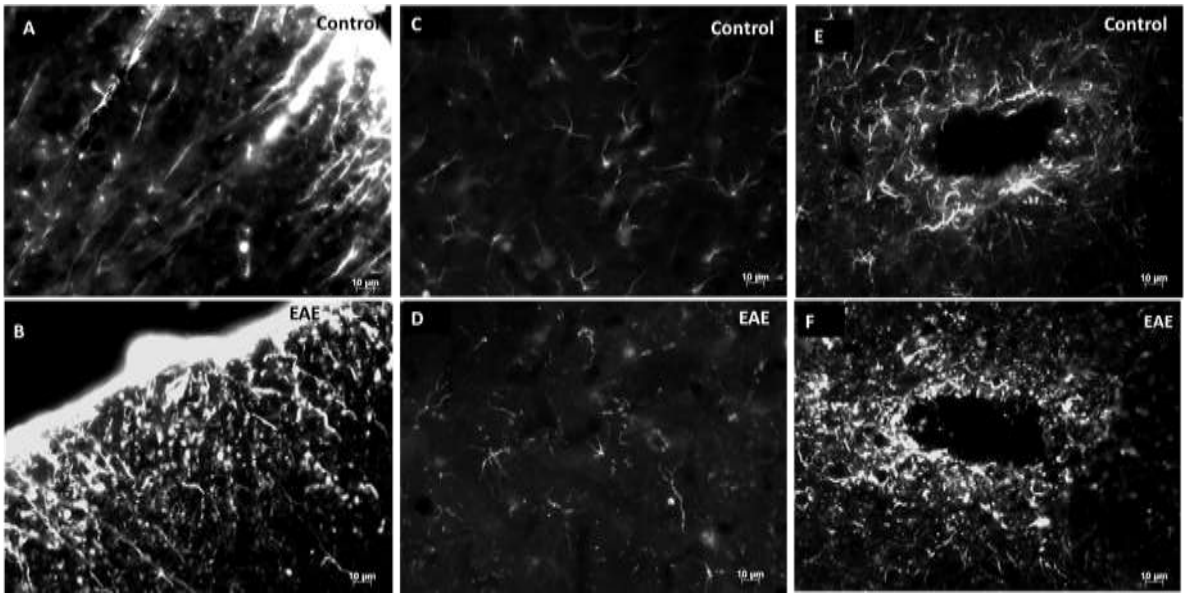

Figure 23- Expression of GFAP at lumbar spinal cord L5-S1 section*. Control immunohistochemistry reaction show GFAP labelled cells with long processes and a wide distribution in analyzed sections (A, C, D). EAE labelled cells appear more condensed and with shorter or none processes in EAE (B, D, F). In EAE animals GFAP labeling tend to be more intense in white matter periphery (B) and near to central canal (F) Images represent this regions from L5-S1 lumbar slices: White matter (A and B), Grey matter (C and D). Central canal (E and F). Scale bar 10 µm.*

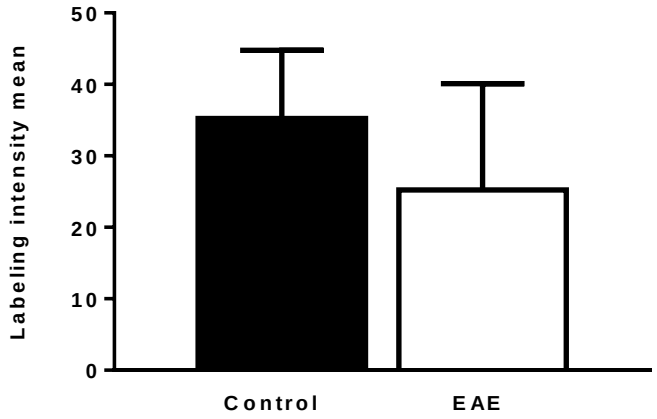

Figure 24-Intensity of GFAP labeled cells expression at ependymal canal of lumbar spinal cord (L5-S1). *Results are expressed as mean ± SD. Were included: n = 3 Control animals; n = 3 EAE animals. Statistical tests: Shapiro-Wilk normality test, followed by a Mann-Whitney test. Shapiro-Wilk test: Data sets do not follow a normal distribution; Mann Whitney test: 'Labeling intensity mean Control vs Labeling intensity mean EAE' No differences were found.*

1.3.5 TRPV1 expression at spinal cord

Spinal expression of TRPV1 was also evaluated in sections from control and EAE rats. Which was found in the superficial layers of the cord. We found a decrease in the expression of this ion channel from 67.4 ± 13.7 in control animals to 54.2 ± 9.54 in EAE group (Figure.25 and 26).

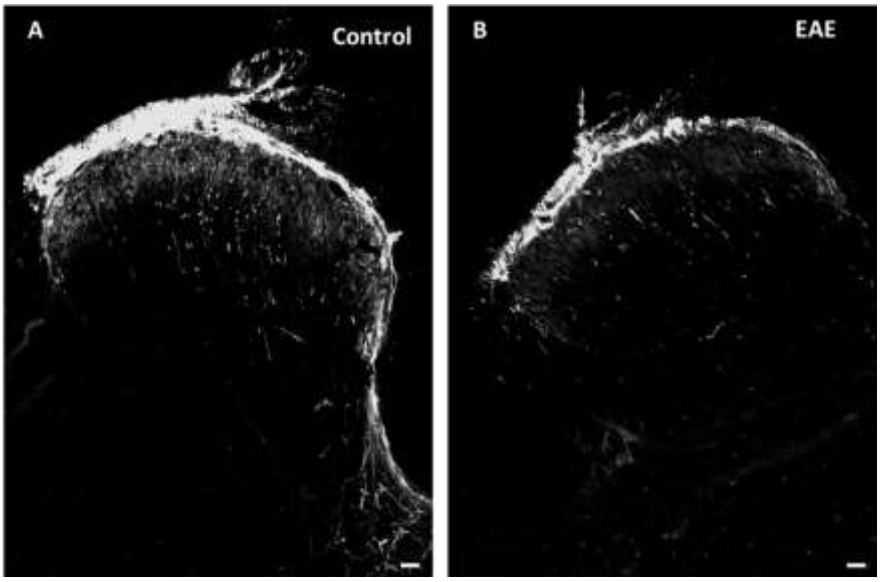

Figure 25- TRPV1 expression at L5-S1 spinal cord sections. *Control animals have high TRPV1 expression when compared to EAE. Scale bar 20 µm.*

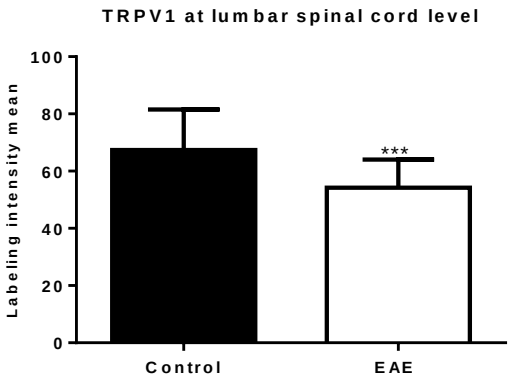

Figure 26- Mean of labelling intensity of TRPV1 at lumbar L5-S1 segments of spinal cord. EAE animals appear with lower mean of TRPV1 intensity labelling (54.2 ± 9.54) when compared to control animals (67.4 ± 13.7). Results are expressed as mean ± SD. Were included: n = 5 Controls; n = 5 EAE Statistical tests: Shapiro-Wilk normality test, followed by a Mann-Whitney test. Shapiro-Wilk test: Data sets don't follow a normal distribution; Mann Whitney test: 'Labeling intensity mean Control vs Labeling intensity mean EAE' ***P = 0.0004.

1.3.6. CGRP and IB4 expression at Spinal Cord

CGRP expression and IB4 binding, respectively markers of peptidergic and non-peptidergic nociceptive afferents, were also studied by immunofluorescence. While CGRP expression was not different between controls and EAE animals (44.0±14.4 and 38.15±10.7, respectively), IB4 binding was significantly reduced from 73.4±23.0 in control animals to 44.3 ±10.01 in EAE rats (Figures 27 and 28).

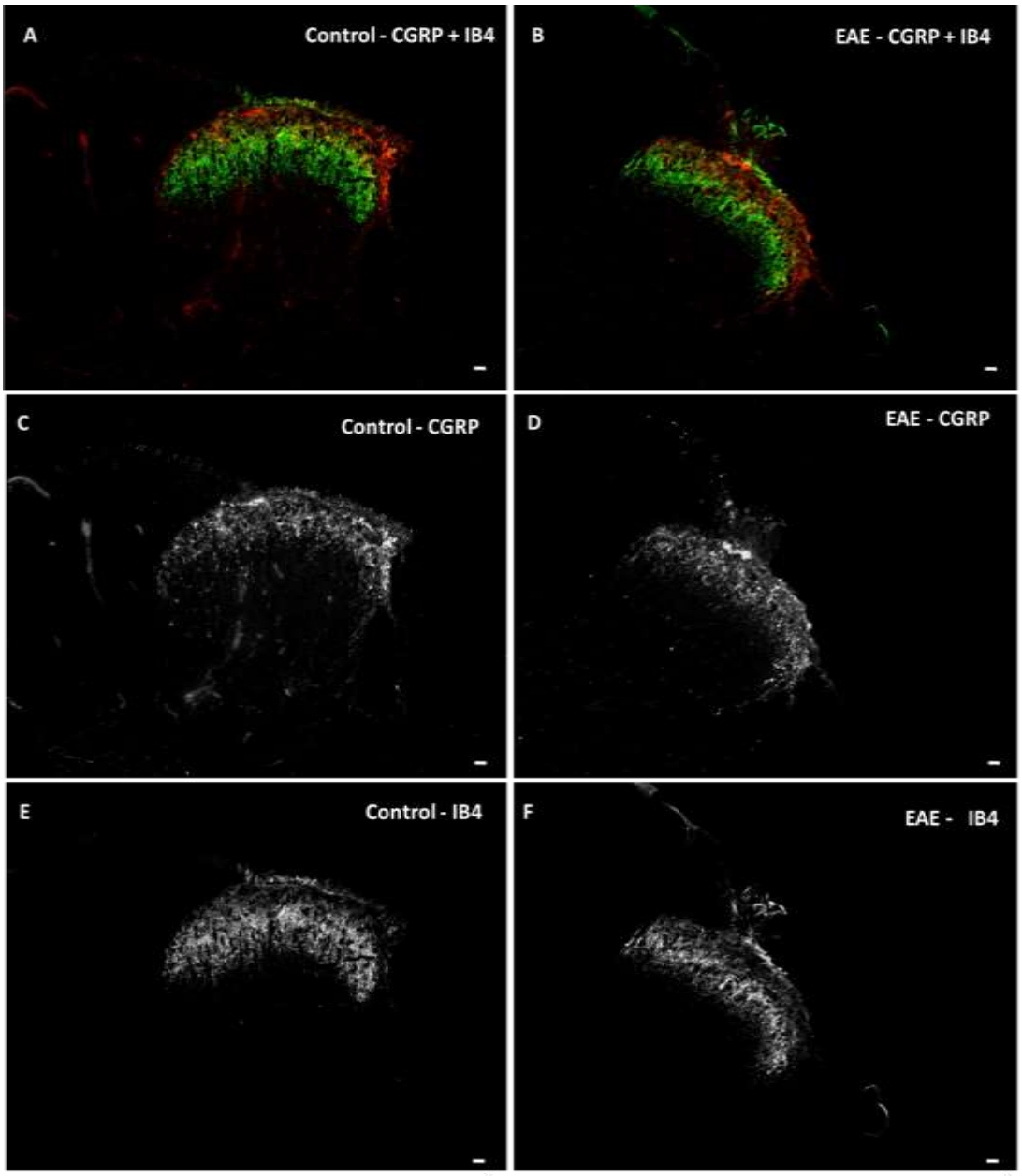

Figure 27- ***CGRP and IB4 immunohistochemistry reaction expression at lumbar spinal cord (L5-S1).*** *No differences were found in CGRP labeling. EAE animals show low IB4 expression at lumbar spinal cord when compared to control animals. Scale bar 20 µm.*

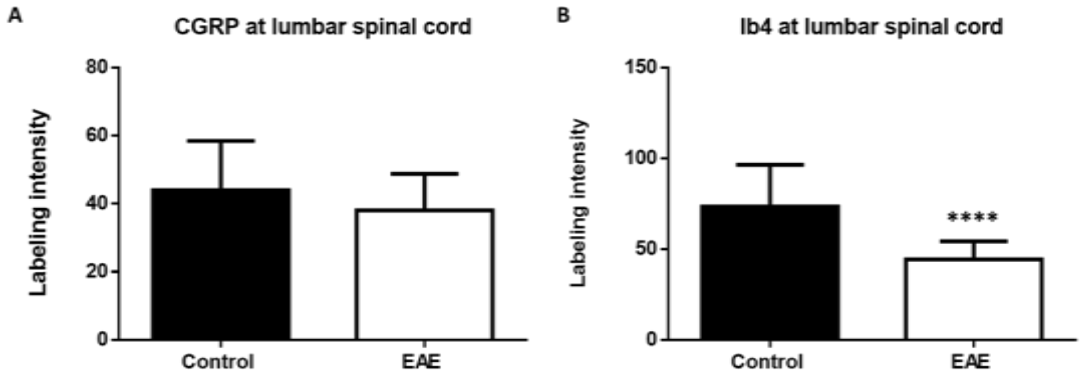

Figure 28- Mean of intensity labeling of CGRP and IB4 at lumbar (L5-S1) spinal cord*. No significant differences were found in EAE CGRP expression (A) IB4 mean intensity labeling was significantly low in EAE rats (B) Results are expressed as mean ± SD. Were included: n = 3 Controls; n = 3 EAE Statistical tests: Shapiro-Wilk normality test, followed by a Mann-Whitney test or a t-test. Shapiro-Wilk test: Data sets for CGRP labeling follow a normal distribution; t-test: 'CGRP labeling intensity mean Control vs CGRP labeling intensity mean EAE' don't show statistic differences. Shapiro-Wilk normality test: Data sets for IB4 follow a normal distribution. Mann-Whitney test 'IB4 labeling intensity Control vs IB4 labeling intensity EAE' ***p <0.0001.*

2. Resiniferatoxin intrathecal injection

2.1 Behaviour results post-RTX injection

2.1.1. Mechanical sensitivity in EAE animals after RTX administration

To investigate the effects of TRPV1 desensitization, RTX was administered on ED 24 and cutaneous sensitivity to mechanical stimuli assessed by the von Frey test, as previously done. In non-treated EAE animals MT was 2.47±1.21g on ED23 and 3.57±2.08g on ED26. In EAE animals receiving intrathecal vehicle, the pre-injection threshold was 2.38±1.29g and 2.01±0.76g after treatment. In EAE animals that received intrathecal RTX, the MT significantly increased from 3.8 ± 1.88 g to 10.67 ± 6.13 g (Figure 29).

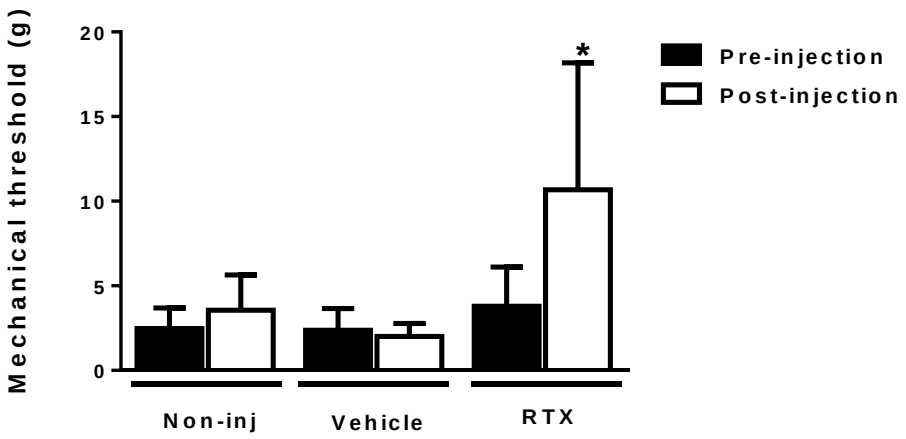

Figure 29- Effects of intrathecal RTX injection in mechanical threshold of EAE animals. *No differences were found in Non-injured animals (EAE) or vehicle (EAE+10% ethanol) between pre or post-injection MTS. MTs of RTX animals (0.1 µg/kg of RTX) show a significant increase post injection. Results are expressed as mean ± SD. Were included: n = 6 'Non-injured', n = 6 'vehicle', n=3 'RTX 0.1 µg/kg' Statistical tests: Shapiro-Wilk normality test, Mann-Whitney test and t-student test. Shapiro-Wilk test – 'with exception of 'RTX 0.1 µg/kg pre-injection' group (Alpha=0.05) none of the others passed normality test. Mann-Whitney test – 'Non-injured pre-injection vs Non-injured post-injection' and 'vehicle pre-injection vs vehicle post-injection' non-significantly different. T-test - 'RTX 0.1 µg/kg pre injection vs RTX 0.1 µg/kg post-injection' *P < 0.05).*

2.1.2. Heat sensitivity in EAE animals after RTX administration

Cutaneous sensitivity to heat was also evaluated, as described above, after RTX. No differences were found between groups in any of the parameters evaluated (Figure 30).

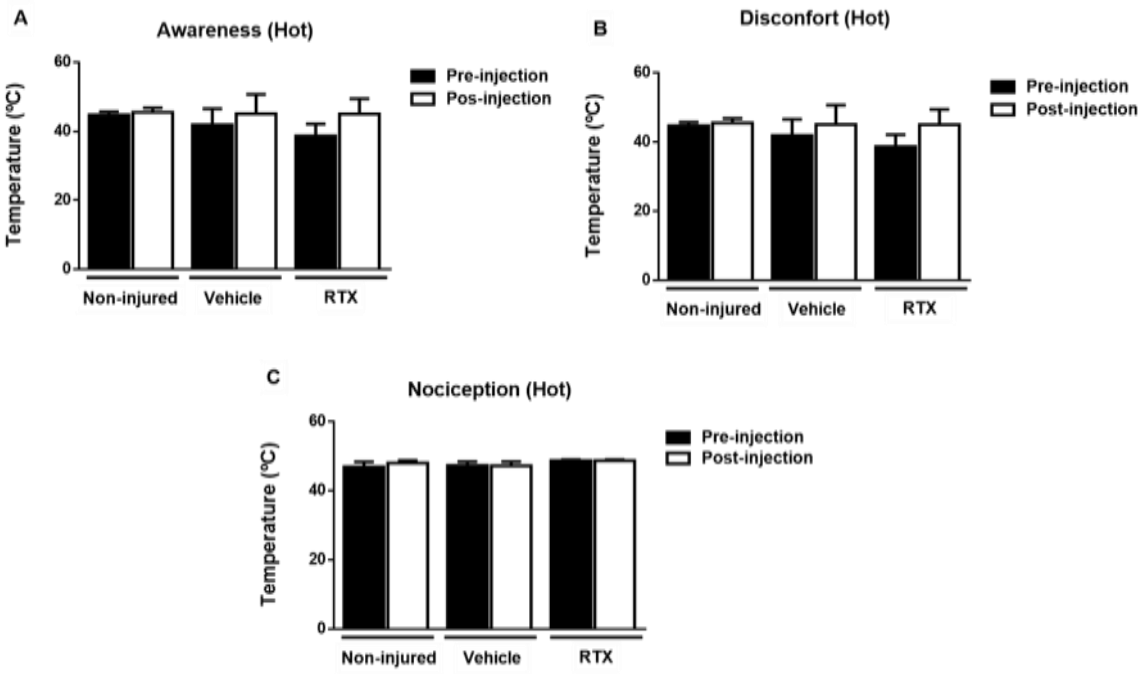

Figure 30- Changes in heat sensitivity after intrathecal RTX injection. *Temperatures of reaction from 'Non-injured', 'Vehicle' and 'RTX 0.1 µg/Kg' to the three evaluated responses, Awareness (A), Discomfort (B) and Nociception (C), pre and post-injection. Results are expressed as mean ± SD. Were included: n = 6 Non-injured (EAE), n = '6 EAE + vehicle intrathecal injection', n=3 'EAE + RTX 0.1 µg/kg intrathecal injection. Statistical tests: Shapiro-Wilk normality test, followed by a t-student test. Shapiro-Wilk test – Alpha=0.05. t-Student test: 'Non-injured pre-injection vs Non injured post-injection'; 'vehicle pre-injection vs vehicle post-injection' non-significantly different; 'RTX 0.1 µg/kg pre injection vs RTX 0,1 µg/kg post-injection' non-significantly different.*

2.1.3. RTX intrathecal injection impact in cold sensitivity of EAE animal

Responses to cold stimulation were also studied, as described above, after RTX. We observed no differences between values recorded before and after intrathecal RTX administration (Figure 31).

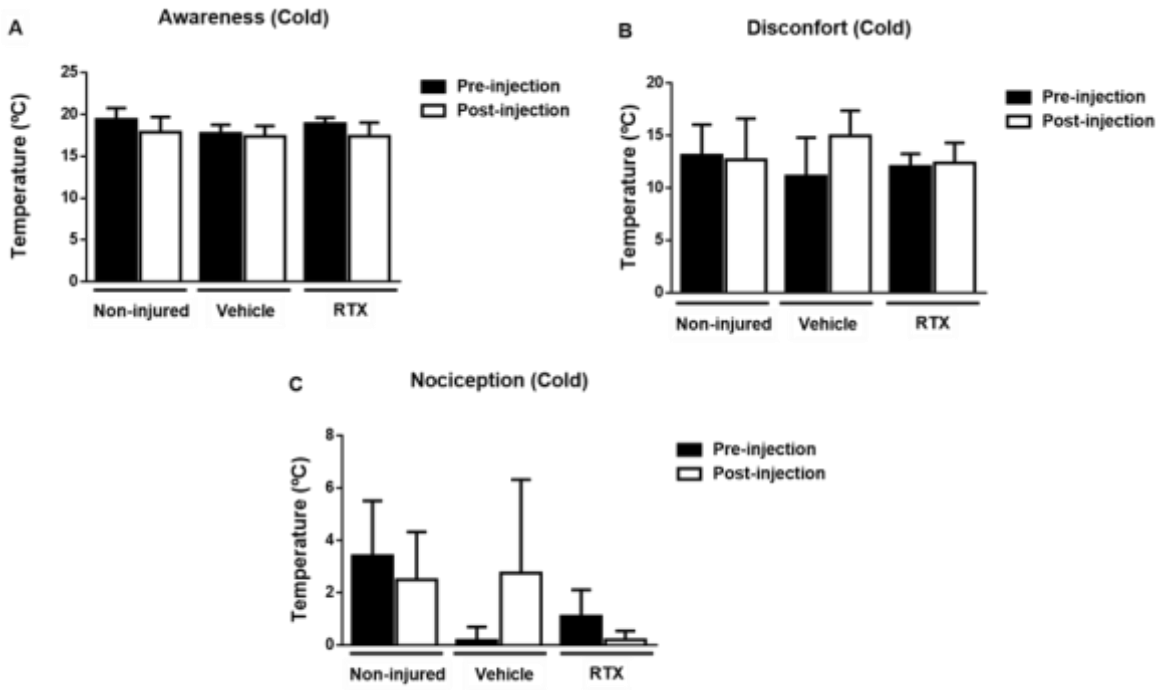

Figure 31- Changes in cold sensitivity upon Intrathecal RTX injection. *Temperatures of reaction from 'Non-injured', 'Vehicle' and 'RTX 0,1 µg/Kg' to the three evaluated responses, Awareness (A), Discomfort (B) and Nociception (C), pre and post-injection. Results are expressed as mean ± SD. Were included: n = 6 Non-injured (EAE), n = '6 EAE + vehicle intrathecal injection', n=7 'EAE + RTX 0.1 µg/kg intrathecal injection. Statistical tests: Shapiro-Wilk normality test, followed by a t-student test. Shapiro-Wilk test (Alpha=0.05). t-Student test: 'vehicle pre-injection vs vehicle post-injection' non-significantly different; 'RTX 0,1 µg/kg pre injection vs 'RTX 0,1 µg/kg post-injection non-significantly different.*

2.2 Bladder function in EAE rats after intrathecal RTX administration

Intrathecal injection of vehicle did not affect bladder reflex activity developed in EAE animals (Figure 32A). The animals injected with vehicle solution presented high frequency of bladder contractions (0.800 ± 0.174 per minute; Figure 33A) with low amplitude (19.8 ± 3.93 cm H2O; Figure 33B), similarly to the initial groups used to describe disease progression. Intrathecal RTX injection improve bladder function of EAE animals, the frequency and amplitude of bladder contraction respectively, being frequency,0.315 ± 0.114 contractions per minute and amplitude 26.2 ± 5.41 cm H2O (Figures 33A and 33B).

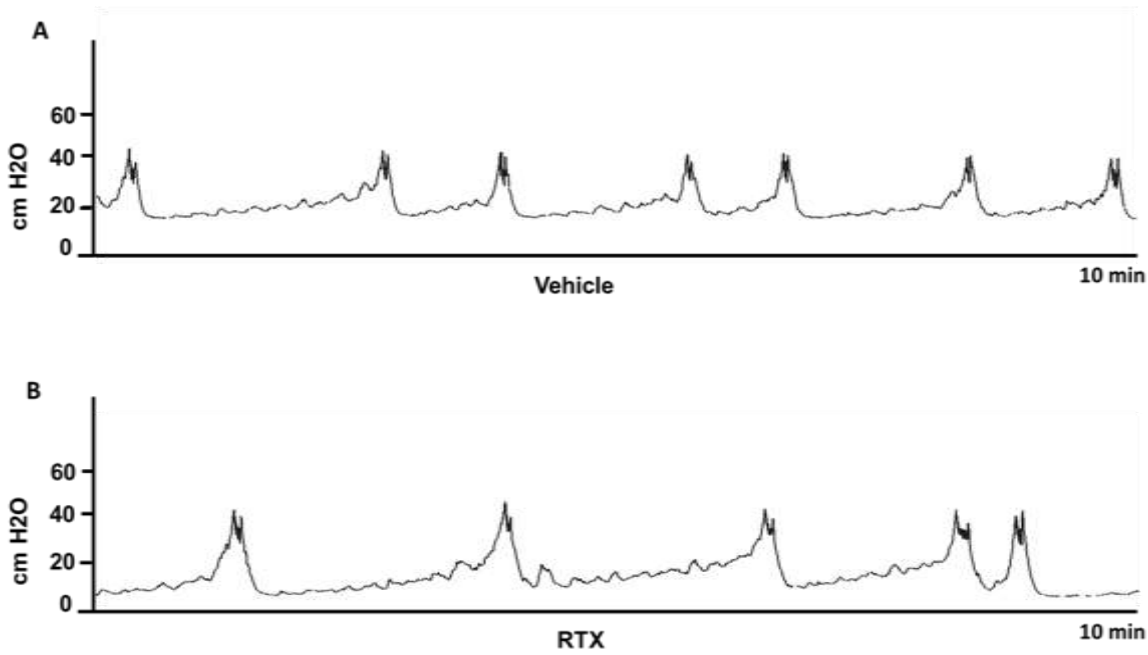

Figure 32- Representative cystometrograms obtained from vehicle and RTX animals. Intrathecal vehicle show high frequency, like previous seen in EAE group), the frequency of contractions being 0.800 ± 0.174 per minute and the amplitude 19.8 ± 3.93 cm H2O (A) Intrathecal RTX animals show low frequency (0.315 ± 0.114) whereas bladder amplitude was not affected (26.3 ± 5.41 cmH2O).

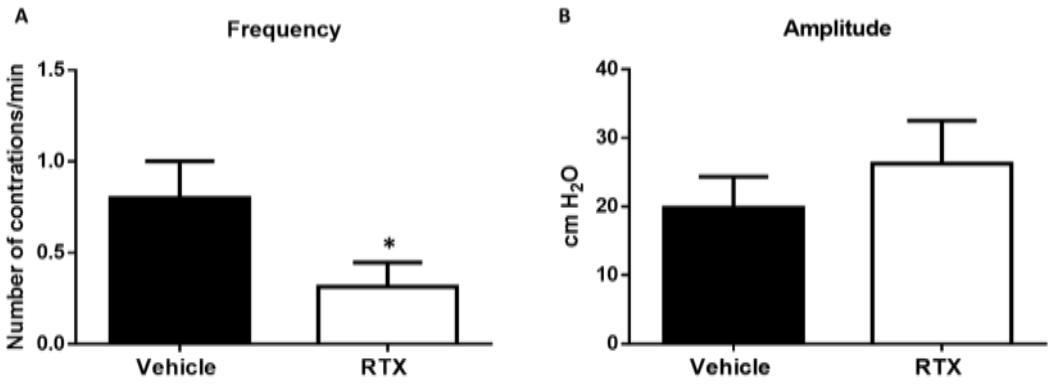

Figure 33- Graph bars depicting the effects in frequency and amplitude upon Vehicle and RTX intrathecal injections. *Upon RTX injection no significate differences were found in amplitude of bladder contractions, despite this, values were high comparing to vehicle (B). The frequency of bladder contractions was significantly decreased by RTX intrathecal injection. (B) Results are expressed as mean ± SD. Were included: n = 6 'vehicle', n=7 'RTX 0, 1 µg/kg' Statistical tests: Shapiro-Wilk normality test, Mann-Whitney test and t-student test. Shapiro-Wilk test – Analysed groups don't passed normality test. Mann-Whitney test – 'Frequency vehicle vs Frequency RTX 0, 1 µg/kg' *p < 0.05; Amplitude vehicle vs Amplitude RTX 0, 1 µg/kg' - statistic differences wasn't found.*

2.3 Spinal effects of intrathecal RTX

2.3.1 C-Fos expression at spinal cord level

As c-Fos is an established marker of spinal nociceptive activation (Coggeshall, 2005; Harris, 1998) and is upregulated after bladder stimulation (Cruz et al., 1996).

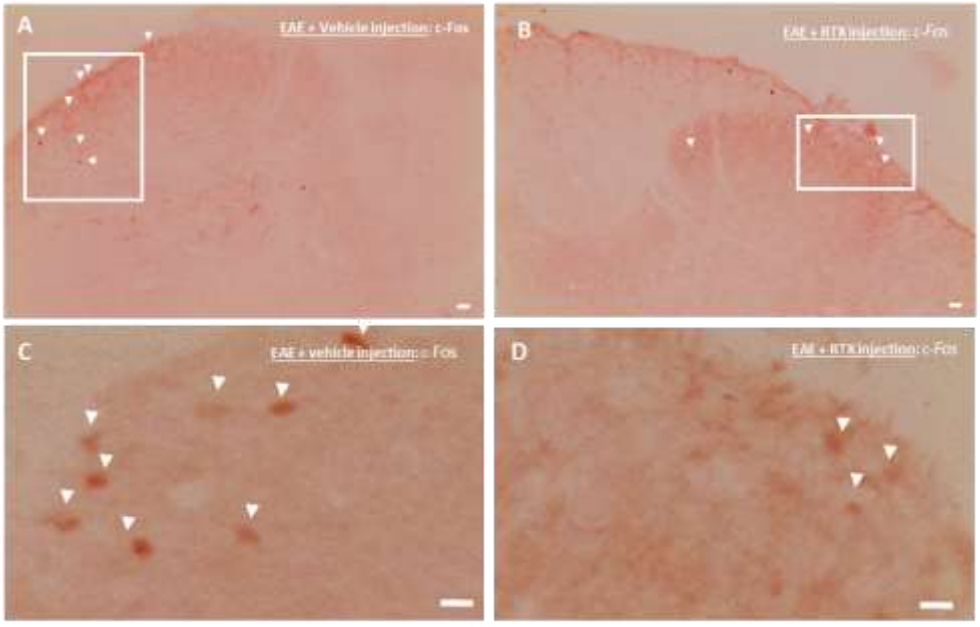

Figure 34- C-Fos expression at dorsal horn of L5-S1 spinal cord sections*. Vehicle injected animals show high number of c-Fos labeled cells at LI and LII (A and C) compared with RTX animals (B and D). Scale bar 20 µm.*

In sections from EAE animals that received intrathecal vehicle, the number of c-Fos positive nuclei, found bilaterally, was 7.38±5.35 in the superficial dorsal horn, 2.27±4.77 in the intermediolateral gray matter (ILGs) and 1.65±3.29 in the dorsal commissure. In sections from RTX-treated EAE rats, the number of immunoreacted nuclei was 4.52±5.96 in the superficial dorsal horn, 0.67±1.46 in the intermediolateral gray matter (ILGs) and 0.48±0.87 in the dorsal commissure (Figure 34 and 35).

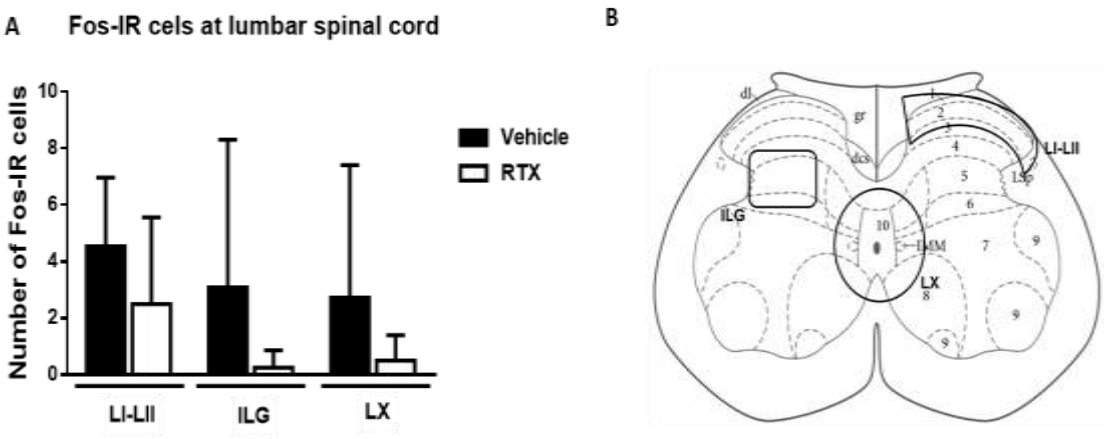

Figure 35- Changes in the number of Fos-IR cells upon Intrathecal RTX injection at lumbar spinal cord*. Animals injected with RTX show less C-Fos marked cells at three analyzed areas, superficial laminae (LI and LII), ILG and LX, when compared with animals injected with vehicle solution (A). Results are expressed as mean ± SD. Were included: n = 6 Non-injured (EAE), n = '6 EAE + vehicle intrathecal injection', n=7 'EAE + RTX 0,1 µg/kg intrathecal injection. Statistical tests: Shapiro-Wilk normality test, followed by a t-student test. Shapiro-Wilk test (Alpha=0.05). t-Student test: 'vehicle pre-injection vs vehicle post-injection' non-significantly different; 'RTX 0,1 µg/kg pre injection vs 'RTX 0,1 µg/kg post-injection non-significantly different****. Schematic representation of analyzed areas to Fos-IR cells****. LI-LII, lamina I and Lamina II; ILG – Intermedial lateral grey matter; LX – Lamina X or central canal (B)*

2.3.2. Spinal TRPV1

Lumbar spinal cord (L5-S1) of animals injected with RTX and vehicle were evaluated. While TRPV1 was present in the superficial layers of the dorsal horn of spinal cord in vehicle-treated EAE rats (111.3 ± 9.91), expression was markedly reduced in sections from RTX-injected animals (12.1 ± 2.77, Figure 36 and 37). Although no measure or statistical analysis were performed, cervical and thoracic levels of spinal cord were observed and TRPV1 expression at this spinal sections was also low comparing to vehicles.

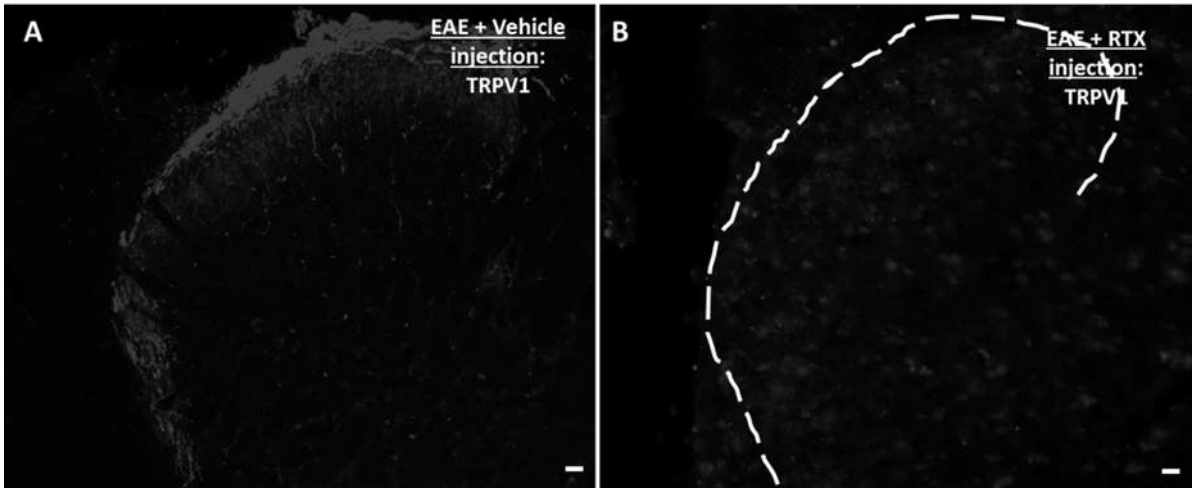

Figure 36- TRPV1 immunohistochemistry expression at L5-S1 spinal cord section. *Intrathecal vehicle injected animals (A) show high TRPV1 expression. In RTX injected animals TRPV1 expression was low (B) comparing to control rats. Scale bar 20 µm.*

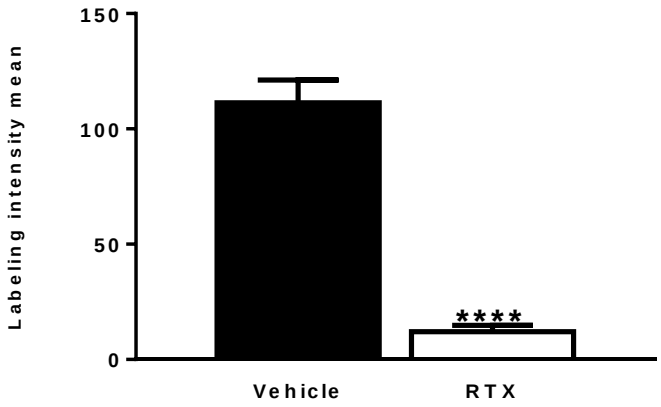

Figure 37- TRPV1 mean labeling intensity post-RTX injection at lumbar L5-S1 segments of spinal cord. *RTX injected animals appear with lower mean of TRPV1 intensity labelling (12.1 ± 2.77) when compared to vehicle animals (111.3 ± 9.91). Results are expressed as mean ± SD. Results are expressed as mean ± SD. Were included: n =3 Controls; n =3 EAE Statistical tests: Shapiro-Wilk normality test, followed by a Mann-Whitney test. Shapiro-Wilk test: Data sets follow a normal distribution; t-test: 'Labeling intensity mean Control vs Labeling intensity mean EAE' ****p <0.0001.*

2.3.3. Iba-1 and GFAP expression at spinal cord level after RTX injection

Immunohistochemistry reactions of sections from vehicle and RTX treated animals show a reduction of Iba-1 intensity labelling and in number of Iba-1 labeled cells. GFAP labeling expression was also low, suggesting an effect of this neurotoxin in spinal glial cells (Figure 38).

The number of iba-1 activated cells at dorsal (13.5±6.20 cells; Figure 39A) and ventral (3.65±3.14 cells; Figure 39B) horn was high in vehicle injected animals comparing to those RTX injected (dorsal horn: 3.65±3.14, ventral horn: 1.17±1.25; Figures 39A and 39B). Intensity of labelling at superficial lamina LI and LII was high in vehicle (20.7±6.98) than in RTX animals (12.1±8.73); Figure 40A. The total cells number at LI and LII of dorsal horn was low in rat injected with the toxin (Vehicle: 34.6±8.16; RTX: 20.5±7.45; Figure 40B). GFAP cells labeling intensity was quantified at central canal of lumbar spinal cord. Results show significant lower intensity labeling in RTX injected animals (15.2±5.44) when compared to controls (24.6± 9.39); Figure 41.

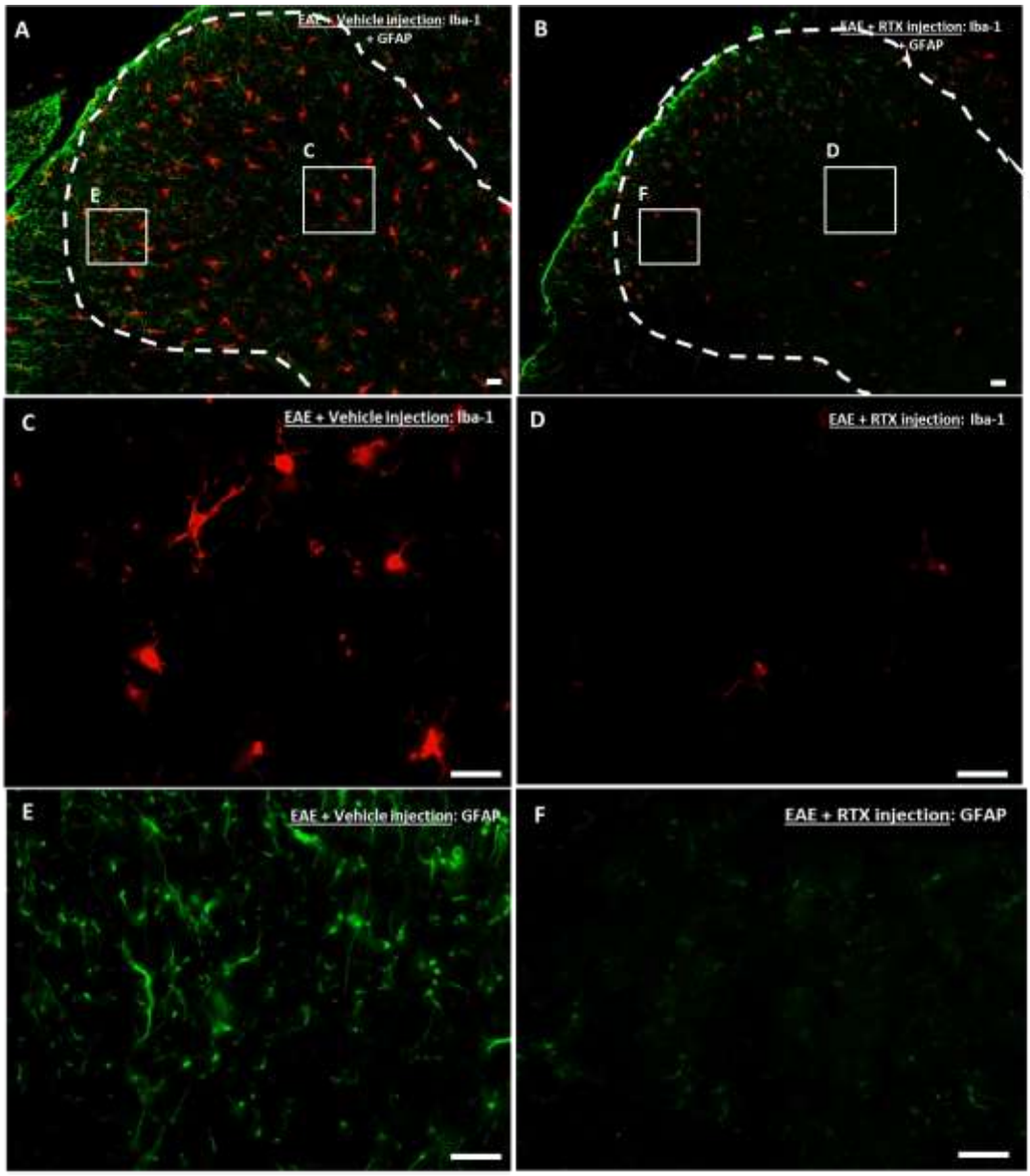

Figure 38- Iba-1 and GFAP expression after vehicle and RTX intrathecal injection. *Vehicle injected animals (A) show activated microglia (cells labelled red) and astrocytes (cells labelled green) at dorsal horn, as amplified in C and E figures respectively. Labeled cells number in vehicle was high comparing to animals injected with RTX (B) that show low glial cells expression, both microglia (D) and astrocytes (F) at dorsal horn of spinal cord and low number of cells.*

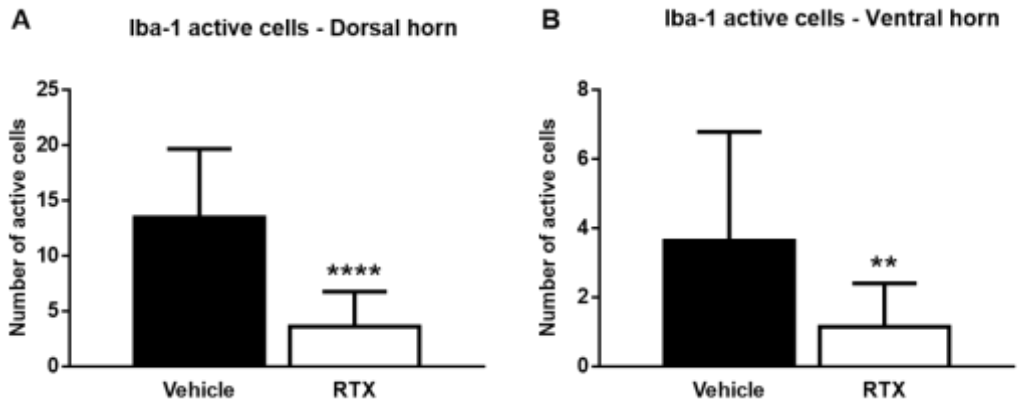

Figure 39 - Number of active microglia after RTX injection. *The number of Iba-1 labeled cells (microglia) was high in vehicle animals, when compared with animals RTX injected, which appear significantly low at dorsal (A) and ventral (B) horns of lumbar (L5-S1) spinal cord. Results are expressed as mean ± SD. Were included: n = 3 Controls; n = 3 EAE Statistical tests: Shapiro-Wilk normality test, followed by a Mann-Whitney test. Shapiro-Wilk test: Data sets do not follow a normal distribution; Mann Whitney test: 'Number of active cells at vehicle dorsal horn vs number of active cells at RTX dorsal horn ****P < 0.0001; 'Number of cells active cells at vehicle ventral horn' v vs Number of active cells at RTX ventral horn' **p<0.05.*

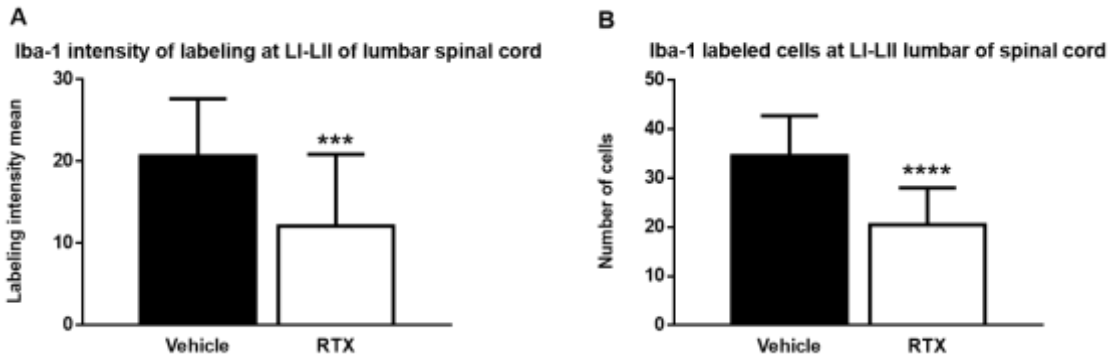

Figure 40 – Intensity and total number of Iba-1 cells at superficial laminas (LI-LII) post RTX injection. *Intensity and number of cells are both significantly decreased in animals RTX injected animals when compared with vehicle animals. Results are expressed as mean ± SD. Were included: n = 3 Controls; n = 3 EAE Statistical tests: Shapiro-Wilk normality test, followed by a Mann-Whitney test or a t-test for those who follow a normal distribution. Shapiro-Wilk test: Data sets do not follow a normal distribution; Mann Whitney test: 'Labeling intensity mean Vehicle' vs 'Labeling intensity mean RTX' ***p= 0.0003; Shapiro-Wilk test: Data sets do follow a normal distribution; t- test: 'Number of cells vehicle' vs 'Number of cells RTX' ****p<0.0001.*

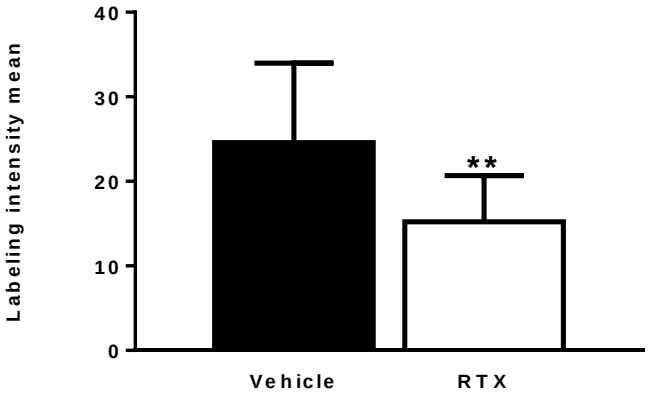

Figure 41 – Intensity of labeling of GFAP post RTX injection. *Mean intensity of labeling was significantly decreased in central canal of RTX injected animals when compared with vehicle animals at lumbar spinal cord (L5-S1). Results are expressed as mean ± SD. Were included: n = 3 Controls; n = 3 EAE Statistical tests: Shapiro-Wilk normality test, followed by t-test Shapiro-Wilk test: Data sets do follow a normal distribution; t- test: 'Labeling intensity mean Vehicle' vs 'Labeling intensity mean RTX' **p= 0.0039.*

V. Discussion

V. Discussion

The present study aimed to investigate the putative role of TRPV1 in pain and bladder dysfunction in EAE, a model for multiple sclerosis disease. For that, we first tested and described the effects of EAE in cutaneous sensitivity and bladder function in Wistar female rats. This was followed by intrathecal administration of RTX or its vehicle in EAE animals and effects on peripheral sensitivity and bladder function documented. Results show that EAE animals developed pain, reflected by increased mechanical and thermal sensitivity. EAE animals also developed bladder dysfunction, characterized by high frequency and low amplitude of bladder reflex contractions. This was accompanied by demyelination in the spinal cord, glial activation, as well as a reduction in peripheral markers, TRPV1 expression and IB4 binding. Intrathecal RTX injection improved pain levels and bladder reflex activity. Results suggests the involvement of the peripheral nervous system to EAE-induced pain and bladder dysfunction. In addition, given the beneficial effects of intrathecal RTX, TRPV1 could be a potential therapeutic target for pain and bladder dysfunction in an EAE model.

1. EAE model - characterization

In the present study we used a variant of the classical EAE model with the addition of periodic cyclosporine injections, according to what had already been described (Thibault et al., 2011) and preliminary testing (Silva et al, unpublished observations). EAE is the most commonly used experimental model for MS and represents a complex condition in which the interaction between a variety of immunopathological and neuropathological mechanisms leads to an approximation of the key pathological features of MS: inflammation, demyelination, axonal loss and gliosis (Popescu et al., 2013). One of the major drawbacks in the EAE model is the difficulty to mimic symptom fluctuation presented by MS patients. In the present study, we found signs

of an increased sensitivity of cutaneous sensitivity to mechanical stimulation and some improvement at early stages of disease progression and at the end of experiments, which is suggestive of a relapsing and remitting form of disease, as reported by Tanuma and coworkers (Tanuma et al., 1999). In that study, the investigators showed that EAE induction accompanied by periodic injections of Cyclosporine A (CsA) is more clinically relevant by inducing a chronic and not an acute form of EAE. Although when given at high doses CsA has immunosuppressive and protective effects (Hess et al., 1988) (Palay et al., 1986) (Paul & Bolton, 1995), at a lower doses CsA helps to mimic MS features in EAE rats, regulating apoptosis of T-cells in the CNS (McCombe et al., 1996) and production of regulatory cytokines (McCombe et al., 1998). Although not seen here, the EAE + CsA model appears to be with more severe in terms of clinical alterations, including motor disturbances, reduced body weight gain and reduced exploratory behavior (Tanuma et al., 1999). Contrary to published reports, the EAE animals assessed in this study did not develop severe clinical symptoms. This could be explained by the higher EAE resistance from Wistar rats when compared to Lewis rats and other strains that have higher susceptibility to develop EAE (Hughes & Stedronska, 1973).

2. Mechanical and Thermal sensation of EAE animals

Chronic pain symptoms in MS are very complex and diverse. While some are directly linked to the disease, other symptoms are indirectly related to MS (Newland et al., 2009). The use of animal models to study MS-related chronic pain syndromes is very limited since only nociceptive component is accessed. Here we investigated the sensory properties of the hindpaws as readout for hyperalgesia and allodynia which constitute one component of MS-related pain. Preliminary observations had established that the EAE model used in this study did not compromise motor function (Silva et al, unpublished observations). It was possible to observe in the EAE group clear signs of pain such as rounded back posture, piloerection, closed eyes and increased mechanical

sensitivity. In addition, we also found behavioral signs of heightened sensitivity to temperatures in the heat range. Sensitivity to both mechanical and thermal stimuli fluctuated, likely mimicking the Human relapsing and remitting MS. In this MS subtype, patients also go through cycles of pain and worsening of loss of motor control, followed by some improvement of their general condition. It is thought this reflects the degradation of central myelin and some neuronal degeneration, followed by some recovery (Furby et al., 2008)

3. Neurogenic detrusor overactivity

While others studies had already documented increased number of voidings and lower bladder amplitude in EAE models (Altuntas et al., 2008; Franken et al., 2015), this is, to our knowledge, the first study to show signs of bladder dysfunction in a Wistar rat strain following EAE induction. Analyses of voiding patterns with filter paper assays indicated signs of bladder dysfunction, which was confirmed by cystometries. We found that EAE animals presented increased frequency and lower amplitude of bladder reflex contractions, resembling NDO in patients with MS. In contrast with other studies in which at least half the animals had detrusor areflexia (Mizusawa et al., 2000; Vignes et al., 2007), we never observed this in the EAE animals studied. In addition, while a previous study has reported a signs of urinary hemorrhage in EAE rats (Lifson et al., 1983), this was never observed during the experimental period. Future studies using this EAE model should include histological analysis of the bladder to confirm the absence of lesions, including ulceration of the urothelium or inflammatory infiltration in the lamina propria. While NDO likely reflects changes in neuronal control related to CNS demyelination, analysis of bladder tissue should help to better characterize MS-related NDO.

4. Spinal changes in EAE

To confirm the molecular mechanisms of EAE, MBP expression was evaluated in the spinal cord and sciatic nerve. As other investigators (Trapp et al., 1998; Trapp & Nave, 2008) we also found a significant reduction in the expression of the myelin protein in the white matter of the cord. Demyelination was restricted to the CNS, as MBP expression was not altered in sciatic nerve sections. In addition, the lack of ATF3 expression is also indicative that EAE only affected the CNS without compromising peripheral innervation. This indicates that the EAE model chosen is able to mimic myelin degradation as seen in MS.

In this study, we found a strong activation of glia cells in the spinal dorsal horn of EAE rats, particularly microglia and astrocytes. It is known that microglia and astrocytes are critical players in the effector phase of EAE and MS (D'Amelio et al., 1990; Kenner et al., 2007) and appear intensively marked in spinal cord and brain over the course of disease (Gray et al., 2008) (Petzold et al., 2002). We found more intense GFAP immunolabelling of astrocytes, which had longer processes, indicative of increased activity. Astrocytes (GFAP) are closely associated with blood vessels (Watson & Frank, 2013), endothelial cells (ECs) and pericytes in BBB, tightly regulating tissue homeostasis in the CNS. We found that GFAP-labeled cells appeared more intensively marked near the white matter and in the grey matter closer to the central canal. We also found evidence of microglial hyperactivation, with more intense Iba1 labelling, shorter and thicker cellular processes and rounded cell bodies. Increased glial activation likely reflects the inflammatory features of MS, in which demyelination is triggered by migration of activated immune cells to the CNS where an auto-immune response is set in motion and myelin degradation takes place (Watson & Frank, 2013). In addition, migrating T-cells release inflammatory cytokines which activate astrocytes and microglial cells. These glial cells also initiate the secretion of other proinflammatory molecules that act on spinal neurons, generating abnormal input, and further heighten glial activation, by acting in an autocrine fashion (Zhang &

An, 2007) This perpetuates CNS inflammation and leads to emergence and maintenance of chronic pain (Cunha *et al.*, 2005; Olechowski *et al.*, 2009) which was observed here during the experimental period.

We also studied the expression of TRPV1 in the spinal cord of EAE rats. As it is well established (Tominaga *et al.*, 1998; Jeffry *et al.*, 2009), TRPV1 was found in the superficial laminae of the cord, where sensory afferents extend their central processes. Studies focusing on neuropathic pain of peripheral origin described an upregulation of TRPV1 expression (Abdullah, 2016; Hudson, 2001; Kanai, 2005). Surprisingly, we observed a decrease in spinal TRPV1. The reasons for this are not clear and further testing is necessary. While it could be speculated if, like other genes (Chow et al., 1999), TRPV1 expression could be regulated by CsA, other studies suggest that CsA is only able to regulate TRPV1 activity by controlling the phosphorylation state of this ion channel (Pearce et al., 2008). Another alternative explanation could reside in peripheral fluctuations of Nerve Growth Factor (NGF), a neurotrophin produced in peripheral tissues that regulates the expression and translation of TRPV1 in sensory neurons (Ji et al., 2002; Bonnington & McNaughton, 2003; Frias et al., 2012), that could impact on TRPV1 expression.

As others have suggested that peripheral sensory neuron injury contributed to pain in EAE mice (Wang et al., 2017), we investigated CGRP expression and IB4 binding, markers of peptidergic and non-peptidergic C-fibres (Basbaum et al., 2009). As in EAE mice (Lu et al., 2012), spinal CGRP expression was not changed. In contrast, we found downregulation of IB4 binding. This is in agreement with other studies that demonstrated a decrease of IB4 labelling of chronic stages of disease (Lu et al., 2012) and suggest the contribution of changes in the peripheral nervous system to MS-induced pain, particularly of unmyelinated C-fibres. Indeed, some studies have documented peripheral changes in both MS patients and EAE animals. For example, in patients there are studies documenting a reduction in peripheral myelin thickness and lower conduction velocity in myelinated nerves (Pollock et al., 1977; Gartzen et al., 2011; Ayromlou et

al., 2013). In experimental animals, signs of myelin loss in peripheral nerves have also been demonstrated (Abdullah, 2016;Misawa, 2008; Sarova-Pinhas, 1995).

5. Effects of intrathecal RTX administration in cutaneous sensitivity and bladder function in EAE animals

RTX is an ultrapotent TRPV1 agonist (Szallasi et al., 2007; Moran et al., 2011) and it has been extensively used to treat chronic pain syndromes and bladder hyperactivity (Avelino et al., 1999; Cruz et al., 2008b; Avelino et al., 2013). The beneficial effects of RTX reflect TRPV1 desensitization, thought to occur in a calcium-dependent manner (Szallasi et al., 2006). RTX is usually administered at the periphery (Avelino et al., 1999; Avelino et al., 2002; Kissin et al., 2005; Abdullah et al., 2016) but studies have demonstrated that intrathecal administration in experimental animals is more effective to treat strong pain and neurogenic detrusor overactivity (Cruz et al., 2008a; Brown et al., 2015; Leo et al., 2017). Here, RTX was intrathecally injected and we found a marked improvement of cutaneous sensitivity to mechanical stimulation and bladder reflex activity, without any effects in sensitivity to thermal stimuli. A marked reduction in spinal TRPV1 was observed following RTX treatment, consistence with TRPV1 desensitization (Cruz et al., 2008a). One indirect evidence of peripheral noxious stimulation is spinal c-Fos expression (Harris, 1998; Coggeshall, 2005), which is strongly reduced after TRPV1 desensitization (Avelino et al., 1999). Accordingly, although results did not reach statistical significance, c-Fos expression in EAE animals that received intrathecal RTX was downregulated.

We also found effects of intrathecal RTX in spinal glial cells, although they were not quantified due to time constraints. Still, we found a reduction in GFAP and Iba1 expression, accompanied by morphological changes, suggesting and effect on astrocytes and microglia, respectively. This could have resulted from a reduction in sensory input caused by RTX treatment. Alternatively, a direct effect of RTX on glial cell might have occurred via TRPV1. Although not tested here, some

authors have reported TRPV1 expression in astrocytes and microglia, in which its activation seems to contribute to central sensitization and other forms of neuroplasticity (Doly *et al.*, 2004; Schilling & Eder, 2009)Altogether, it seems likely that TRPV1 could serve as an attractive therapeutic target to be blocked by either desensitizing agonists or specific antagonists and improve pain and bladder function (Cruz et al., 2008c; Gunthorpe & Szallasi, 2008; Charrua et al., 2009).

VI. Conclusions and Future perspectives

VI. Conclusions and Future perspectives

The present study was designed to implement an EAE model that could be further used to test treatments and unravel mechanisms of disease. Particularly, we aimed to test if TRPV1 was important for pain and bladder dysfunction associated with EAE, serving as a putative therapeutic target. We were successful in establishing an EAE model with fluctuation in cutaneous sensitivity, reminiscent of the relapsing-remitting forms of MS. In addition, EAE animals also had marked bladder dysfunction, which resembled NDO present in most MS patients. At a cellular level, we found evidence of demyelination, restricted to the central nervous system, and activation of glial cells, known to be key players in neuropathic pain. Moreover, changes in peripheral markers of sensory afferents (TRPV1, CGRP and IB4 binding) suggest a contribution of the peripheral nervous system to pain and abnormal pain reflex activity in EAE rats. Intrathecal RTX administration improved cutaneous sensitivity and bladder function. This was accompanied by a reduction in spinal TRPV1 expression, indicative of receptor desensitization, and diminished activation of astrocytes microglial cells. This strongly suggests that TRPV1 is a key player in pain and bladder dysfunction arising in EAE and could serve as a therapeutic target for MS.

Although interesting, this study presents limitations and paves the way for further analysis:

- As we did not observe any major impairment, we conclude that EAE induced was very mild, which may make results observed here more difficult to translate to a clinical context. It is relevant to extend these results to a more aggressive model.

- Pain and bladder dysfunction likely results from demyelination occurring at the spinal cord, the same should have occurred in supraspinal centers. Thus, we propose to evaluate MBP expression in supraspinal structures involved in pain processing and bladder control, including the pontine micturition center, periaqueductal nucleus and A5 area.

- Immunohistochemical analysis is incomplete in this study due to time constraints. Hence, expression of TRPV1, CGRP and IB4 binding should be evaluated in DRG and peripheral tissues, including the bladder and hindpaw skin. Moreover, quantification of MBP expression in the sciatic nerve as well as TRPv1, Iba1, GFAP after RTX treatment should be concluded.

- As the degree of glial activation was increased in EAE and reduced following RTX, spinal levels of pro-inflammatory cytokines released by these cells should be measured.

- Importantly, increased permeability of BBB is a key established feature of EAE and MS, allowing the migration of activate immune cells to the CNS that initiate myelin degradation. It was not evaluated in the present study but should be done in the future.

- Although our results suggest that TRPV1 manipulation could have therapeutic relevance, it remains to be established if it also contributes to disease initiation. Future studies could test if pre-emptive intrathecal administration could prevent EAE in rats.

VII. References

Abdullah, M., Mahowald, M.L., Frizelle, S.P., Dorman, C.W., Funkenbusch, S.C. & Krug, H.E. (2016) The effect of intra-articular vanilloid receptor agonists on pain behavior measures in a murine model of acute monoarthritis. J Pain Res, 9, 563-570.

Altuntas, C.Z., Daneshgari, F., Liu, G., Fabiyi, A., Kavran, M., Johnson, J.M., Gulen, M.F., Jaini, R., Li, X., Frenkl, T.L. & Tuohy, V.K. (2008) Bladder dysfunction in mice with experimental autoimmune encephalomyelitis. J Neuroimmunol, 203, 58-63.

Avelino, A., Charrua, A., Frias, B., Cruz, C., Boudes, M., de Ridder, D. & Cruz, F. (2013) Transient receptor potential channels in bladder function. Acta Physiol (Oxf), 207, 110-122.

Avelino, A., Cruz, C., Nagy, I. & Cruz, F. (2002) Vanilloid receptor 1 expression in the rat urinary tract. Neuroscience, 109, 787-798.

Avelino, A., Cruz, F. & Coimbra, A. (1999) Intravesical resiniferatoxin desensitizes rat bladder sensory fibres without causing intense noxious excitation. A c-fos study. Eur J Pharmacol, 378, 17-22.

Ayromlou, H., Mohammad-Khanli, H., Yazdchi-Marandi, M., Rikhtegar, R., Zarrintan, S., Golzari, S.E. & Ghabili, K. (2013) Electrodiagnostic evaluation of peripheral nervous system changes in patients with multiple sclerosis. Malays J Med Sci, 20, 32-38.

Basbaum, A.I., Bautista, D.M., Scherrer, G. & Julius, D. (2009) Cellular and molecular mechanisms of pain. Cell, 139, 267-284.

Bonnington, J.K. & McNaughton, P.A. (2003) Signalling pathways involved in the sensitisation of mouse nociceptive neurones by nerve growth factor. The Journal of physiology, 551, 433-446.

Brown, D.C., Agnello, K. & Iadarola, M.J. (2015) Intrathecal resiniferatoxin in a dog model: efficacy in bone cancer pain. Pain, 156, 1018-1024.

Charrua, A., Cruz, C.D., Narayanan, S., Gharat, L., Gullapalli, S., Cruz, F. & Avelino, A. (2009) GRC-6211, a new oral specific TRPV1 antagonist, decreases bladder overactivity and noxious bladder input in cystitis animal models. J Urol, 181, 379-386.

Chow, C.W., Rincon, M. & Davis, R.J. (1999) Requirement for transcription factor NFAT in interleukin-2 expression. Mol Cell Biol, 19, 2300-2307.

Coggeshall, R.E. (2005) Fos, nociception and the dorsal horn. Progress in neurobiology, 77, 299-352.

Cruz, C.D., Charrua, A., Vieira, E., Valente, J., Avelino, A. & Cruz, F. (2008a) Intrathecal delivery of resiniferatoxin (RTX) reduces detrusor overactivity and spinal expression of TRPV1 in spinal cord injured animals. Exp Neurol, 214, 301-308.

Cruz, F., Charrua, A., Cruz, C., Gharat, L., Gullapalli, S., Narayanan, S. & Avelino, A. (2008b) GRC 6211, a new oral TRPV1 antagonist, decreases the frequency of bladder reflex contractions and noxious input in rats with acute or chronic cystitis. European Urology Supplements, 7, 181-181.

Cruz, F., Charrua, A., Cruz, C., Narayanan, S., Gharat, L., Gullapalli, S. & Avelino, A. (2008c) The oral TRPV1 antagonist GRC 6211 reduces bladder overactivity and noxious bladder input in cystitis. Journal of Urology, 179, 539-539.

Cunha, T.M., Verri, W.A., Jr., Silva, J.S., Poole, S., Cunha, F.Q. & Ferreira, S.H. (2005) A cascade of cytokines mediates mechanical inflammatory hypernociception in mice. Proc Natl Acad Sci U S A, 102, 1755-1760.

D'Amelio, F.E., Smith, M.E. & Eng, L.F. (1990) Sequence of tissue responses in the early stages of experimental allergic encephalomyelitis (EAE): immunohistochemical, light microscopic, and ultrastructural observations in the spinal cord. Glia, 3, 229-240.

Doly, S., Fischer, J., Salio, C. & Conrath, M. (2004) The vanilloid receptor-1 is expressed in rat spinal dorsal horn astrocytes. Neuroscience letters, 357, 123-126.

Franken, J., Gevaert, T., Uvin, P., Wauterickx, K., Boeve, A.C., Rietjens, R., Boudes, M., Hendriks, J.J., Hellings, N., Voets, T. & De Ridder, D. (2015) Urodynamic changes in mice with experimental autoimmune encephalomyelitis correlate with neurological impairment. Neurourology and urodynamics.

Frias, B., Charrua, A., Avelino, A., Michel, M.C., Cruz, F. & Cruz, C.D. (2012) Transient receptor potential vanilloid 1 mediates nerve growth factor-induced bladder hyperactivity and noxious input. BJU Int.

Gartzen, K., Katzarava, Z., Diener, H.C. & Putzki, N. (2011) Peripheral nervous system involvement in multiple sclerosis. European journal of neurology : the official journal of the European Federation of Neurological Societies, 18, 789-791.

Gray, E., Thomas, T.L., Betmouni, S., Scolding, N. & Love, S. (2008) Elevated activity and microglial expression of myeloperoxidase in demyelinated cerebral cortex in multiple sclerosis. Brain Pathol, 18, 86-95.

Gunthorpe, M.J. & Szallasi, A. (2008) Peripheral TRPV1 receptors as targets for drug development: new molecules and mechanisms. Curr Pharm Des, 14, 32-41.

Harris, J.A. (1998) Using c-fos as a neural marker of pain. Brain Res Bull, 45, 1-8.

Hess, A.D., Esa, A.H. & Colombani, P.M. (1988) Mechanisms of action of cyclosporine: effect on cells of the immune system and on subcellular events in T cell activation. Transplant Proc, 20, 29-40.

Hudson, L.J., Bevan, S., Wotherspoon, G., Gentry, C., Fox, A. & Winter, J. (2001) VR1 protein expression increases in undamaged DRG neurons after partial nerve injury. Eur J Neurosci, 13, 2105-2114.

Hughes, R.A. & Stedronska, J. (1973) The susceptibility of rat strains to experimental allergic encephalomyelitis. Immunology, 24, 879-884.

Jeffry, J.A., Yu, S.Q., Sikand, P., Parihar, A., Evans, M.S. & Premkumar, L.S. (2009) Selective targeting of TRPV1 expressing sensory nerve terminals in the spinal cord for long lasting analgesia. PLoS One, 4, e7021.

Ji, R.R., Samad, T.A., Jin, S.X., Schmoll, R. & Woolf, C.J. (2002) p38 MAPK activation by NGF in primary sensory neurons after inflammation increases TRPV1 levels and maintains heat hyperalgesia. Neuron, 36, 57-68.

Kanai, Y., Nakazato, E., Fujiuchi, A., Hara, T. & Imai, A. (2005) Involvement of an increased spinal TRPV1 sensitization through its up-regulation in mechanical allodynia of CCI rats. Neuropharmacology, 49, 977-984.

Kenner, M., Menon, U. & Elliott, D.G. (2007) Multiple sclerosis as a painful disease. Int Rev Neurobiol, 79, 303-321.

Kissin, E.Y., Freitas, C.F. & Kissin, I. (2005) The effects of intraarticular resiniferatoxin in experimental knee-joint arthritis. Anesth Analg, 101, 1433-1439.

Leo, M., Schulte, M., Schmitt, L.I., Schafers, M., Kleinschnitz, C. & Hagenacker, T. (2017) Intrathecal Resiniferatoxin Modulates TRPV1 in DRG Neurons and Reduces TNF-Induced Pain-Related Behavior. Mediators Inflamm, 2017, 2786427.

Lifson, J.D., Oyasu, R., Dreyer, N., Carone, F.A. & Williams, R.M. (1983) Acute hemorrhagic obstructive uropathy as a complication of experimental autoimmune encephalomyelitis. Arch Pathol Lab Med, 107, 600-602.

Lu, J., Kurejova, M., Wirotanseng, L.N., Linker, R.A., Kuner, R. & Tappe-Theodor, A. (2012) Pain in experimental autoimmune encephalitis: a comparative study between different mouse models. J Neuroinflammation, 9, 233.

McCombe, P.A., Nickson, I. & Pender, M.P. (1998) Cytokine expression by inflammatory cells obtained from the spinal cords of Lewis rats with experimental autoimmune encephalomyelitis induced by inoculation with myelin basic protein and adjuvants. J Neuroimmunol, 88, 30-38.

McCombe, P.A., Nickson, I., Tabi, Z. & Pender, M.P. (1996) Apoptosis of V beta 8.2+ T lymphocytes in the spinal cord during recovery from experimental autoimmune encephalomyelitis induced in Lewis rats by inoculation with myelin basic protein. J Neurol Sci, 139, 1-6.

Misawa, S., Kuwabara, S., Mori, M., Hayakawa, S., Sawai, S. & Hattori, T. (2008) Peripheral nerve demyelination in multiple sclerosis. Clin Neurophysiol, 119, 1829-1833.

Mizusawa, H., Igawa, Y., Nishizawa, O., Ichikawa, M., Ito, M. & Andersson, K.E. (2000) A rat model for investigation of bladder dysfunction associated with demyelinating disease resembling multiple sclerosis. Neurourology and urodynamics, 19, 689-699.

Moran, M.M., McAlexander, M.A., Biro, T. & Szallasi, A. (2011) Transient receptor potential channels as therapeutic targets. Nature reviews. Drug discovery, 10, 601-620.

Newland, P.K., Naismith, R.T. & Ullione, M. (2009) The impact of pain and other symptoms on quality of life in women with relapsing-remitting multiple sclerosis. J Neurosci Nurs, 41, 322-328.

Olechowski, C.J., Truong, J.J. & Kerr, B.J. (2009) Neuropathic pain behaviours in a chronic-relapsing model of experimental autoimmune encephalomyelitis (EAE). Pain, 141, 156-164.

Palay, D.A., Cluff, C.W., Wentworth, P.A. & Ziegler, H.K. (1986) Cyclosporine inhibits macrophage-mediated antigen presentation. J Immunol, 136, 4348-4353.

Paul, C. & Bolton, C. (1995) Inhibition of blood-brain barrier disruption in experimental allergic encephalomyelitis by short-term therapy with dexamethasone or cyclosporin A. Int J Immunopharmacol, 17, 497-503.

Pearce, L.V., Toth, A., Ryu, H., Kang, D.W., Choi, H.K., Jin, M.K., Lee, J. & Blumberg, P.M. (2008) Differential modulation of agonist and antagonist structure activity relations for rat TRPV1 by cyclosporin A and other protein phosphatase inhibitors. Naunyn Schmiedebergs Arch Pharmacol, 377, 149-157.

Petzold, A., Eikelenboom, M.J., Gveric, D., Keir, G., Chapman, M., Lazeron, R.H., Cuzner, M.L., Polman, C.H., Uitdehaag, B.M., Thompson, E.J. & Giovannoni, G. (2002) Markers for different glial cell responses in multiple sclerosis: clinical and pathological correlations. Brain, 125, 1462-1473.

Pollock, M., Calder, C. & Allpress, S. (1977) Peripheral nerve abnormality in multiple sclerosis. Ann Neurol, 2, 41-48.

Popescu, B.F., Pirko, I. & Lucchinetti, C.F. (2013) Pathology of multiple sclerosis: where do we stand? Continuum (Minneap Minn), 19, 901-921.

Sarova-Pinhas, I., Achiron, A., Gilad, R. & Lampl, Y. (1995) Peripheral neuropathy in multiple sclerosis: a clinical and electrophysiologic study. Acta Neurol Scand, 91, 234-238.

Schilling, T. & Eder, C. (2009) Importance of the non-selective cation channel TRPV1 for microglial reactive oxygen species generation. Journal of neuroimmunology, 216, 118-121.

Szallasi, A., Cortright, D.N., Blum, C.A. & Eid, S.R. (2007) The vanilloid receptor TRPV1: 10 years from channel cloning to antagonist proof-of-concept. Nature reviews. Drug discovery, 6, 357-372.

Szallasi, A., Cruz, F. & Geppetti, P. (2006) TRPV1: a therapeutic target for novel analgesic drugs? Trends Mol Med, 12, 545-554.

Tanuma, N., Shin, T., Kogure, K. & Matsumoto, Y. (1999) Differential role of TNF-alpha and IFN-gamma in the brain of rats with chronic relapsing autoimmune encephalomyelitis. J Neuroimmunol, 96, 73-79.

Thibault, K., Calvino, B. & Pezet, S. (2011) Characterisation of sensory abnormalities observed in an animal model of multiple sclerosis: a behavioural and pharmacological study. Eur J Pain, 15, 231 e231-216.

Tominaga, M., Caterina, M.J., Malmberg, A.B., Rosen, T.A., Gilbert, H., Skinner, K., Raumann, B.E., Basbaum, A.I. & Julius, D. (1998) The cloned capsaicin receptor integrates multiple pain-producing stimuli. Neuron, 21, 531-543.

Vignes, J.R., Deloire, M.S., Petry, K.G. & Nagy, F. (2007) Characterization and restoration of altered inhibitory and excitatory control of micturition reflex in experimental autoimmune encephalomyelitis in rats. J Physiol, 578, 439-450.

Wang, I.C., Chung, C.Y., Liao, F., Chen, C.C. & Lee, C.H. (2017) Peripheral sensory neuron injury contributes to neuropathic pain in experimental autoimmune encephalomyelitis. Sci Rep, 7, 42304.

Watson, A.J. & Frank, M.G. (2013) Astrocytes do the "shuttle". Sleep, 36, 1413-1414.